CH-83
CONDOR

A Design Solution to Satisfy the Expeditionary Warfare Vertical Heavy Lift Requirement

NAVAL POSTGRADUATE SCHOOL HELICOPTER DESIGN TEAM
MARCH 2003

2003 *CONDOR* Design Team Members

ENS Ben Carter, USN _____

ENS John Ciaravino, USN _____

MAJ Choon Lim, RSAF _____

ENS Jason Papadopoulos, USN _____

ENS Matt Rodgers, USN _____

CPT Michael Tan, RSAF _____

MAJ Steven Van Riper, USA _____

Dr. E. Roberts Wood _____
(Faculty Advisor)

Dr. James Mar _____
(Faculty Advisor)

CH-83 *Condor* Executive Summary

The next generation ship based military heavy lift rotorcraft must be a versatile aircraft capable of conducting long-range combat assaults in support of full spectrum combat operations. It must be capable of operating in all weather conditions, day or night, from prepared or unprepared surfaces. The design must offer commonality with current use aircraft and technical compatibility with legacy aircraft and supporting ground equipment. The design must offer an aircraft that is economically feasible to produce, procure and operate.

The helicopter design contained in this proposal meets or exceeds all of the requirements of the Operational Requirements Document (ORD) and the needs of the United States Marine Corps. The design emphasizes factors that are essential to military mission accomplishment and maintainability but the potential exist for a variant of the design to be used for civilian commuter and cargo service.

Parametric studies were conducted based on the mission profiles contained in the ORD. The results of the studies were used to ascertain what general performance attributes would be required in order to accomplish the given missions. An evaluation criterion matrix was used to determine the optimum configuration, which turned out to be a winged, single rotor helicopter with auxiliary propulsion named CH-83 *Condor*. The *Condor* is not a radical design although it does rely on a technology currently in development by the Sikorsky Aircraft Corporation called Reverse Velocity Rotor (RVR).

The *Condor* is a quad-engine, rear loading, single rotor helicopter which utilizes an optimally sized wing to unload the main rotor during high speed flight. The aircraft retains all the low speed handling qualities of a traditional helicopter but reaps all the benefits of a fixed wing cargo aircraft at cruise speed, with the wing providing nearly 80% of the lift.

Maximum range under mission conditions is 615 nautical miles. Maximum gross weight is 120,000 lbs. Maximum cargo capacity is 37,500 lbs. Each of the four engines has a maximum power rating of 6,150 shaft horsepower. The rotor system is an eight bladed (110 foot diameter), fully articulated, foldable system with each blade incorporating the RVR airfoil cross section. The rotor system is driven by a lightweight variable speed transmission that allows RPM modulate between 50% and 100% of operating RPM based on flight mode. The anti-torque system is a traditional six bladed tail rotor mounted to the vertical stabilizer. Auxiliary propulsion is provided by two propellers (fifteen foot diameter), each mated to one of the powerplants and

mounted on each wing. *Condor* is a fully digital helicopter, incorporating an advanced computer controlled 1P plus 2P control system to accommodate the RVR system, a glass cockpit with conventional flight controls and fly-by-wire technology, and full authority digital engine control.

The cargo 'box' of the aircraft is multi-mission configurable with provisions for everything from troop transport to heavy equipment resupply. Two load masters will be able to load and unload pallets, secure vehicles, and configure almost any outsize cargo arrangement via embedded cargo handling systems. The *Condor* is fitted with a single external load hook capable of single point lifts up to 12,000 lbs.

Although the aircraft is compatible with current LHA and LHD flight decks it is purpose designed for the next generation of large amphibious assault ship. Each of these next generation ships will be able to berth four *Condors*, maintenance personnel, and required ground support equipment.

The *Condor* is fully capable of long range self-deployment using either in-flight refueling or internal auxiliary fuel tanks mounted in the cargo compartment.

TABLE OF CONTENTS

LIST OF FIGURES

LIST OF TABLES

1. INTRODUCTION

In June 2002, the Total Ship Systems Engineering design team submitted initial requirements for a long range, heavy lift aircraft to support Marine Corps, joint, and coalition force operations ashore up to 200 nm inland in a forcible entry environment. The aircraft was intended to operate from ships of the amphibious task force, specifically the Amphibious Assault and Logistics Support variants of the family of expeditionary warfare platforms currently under design by the Total Ship Systems Engineering curriculum.

1.1 REQUIREMENTS

The basic requirements were for the aircraft to have a minimum of 300 nm radius of action and to carry a minimum of 37,500 lbs of payload. The aircraft was also desired to cruise at speeds in excess of 200 knots in order to minimize transit time.

Long Range Heavy Lift Aircraft Mission Profile

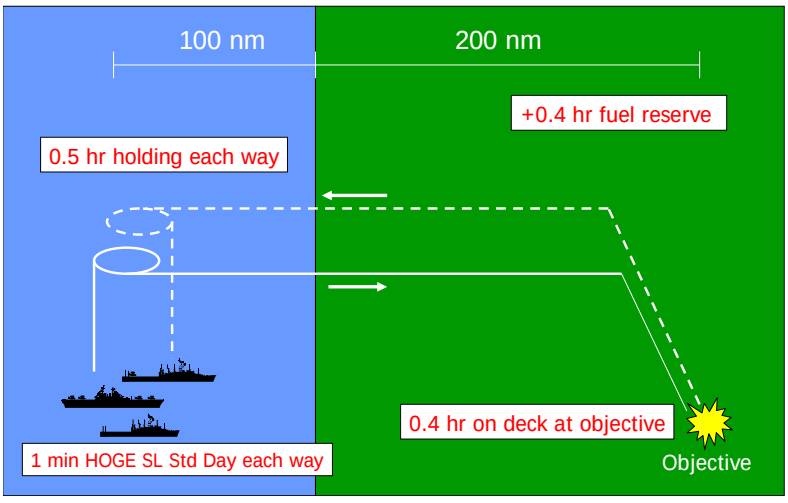

Figure 1.1.1: Typical Mission Profile

In addition, the system was allowed to have, as a maximum, a spot factor no larger than twice that of the CH-53E (threshold), but preferable a spot factor no more than 1.5 times that of the CH-53E. This spot factor requirement applied to both spread and folded configurations.

Expeditionary Warfare payload requirements provided the basis for design of the concept fuselage. System level requirements for payload included:

Capable of transporting equipment as large as an LAV or MTVR variant supporting the new lightweight 155 mm howitzer. Handling 8’ x 8’ x 20’ and 8’ x 8’ x 40’ standard shipping containers (weighing no more than 37,500 lbs), as well as a pair of 8’ x 8’ x 5’ “quadcons” (weighing no more than 37,500 lbs total).

1.2 PRELIMINARY DESIGN STUDIES

Initially, the Aeronautical Engineering design team attempted to look at all possible options. All of the options were grouped into five categories: helicopter, compound helicopter, tilt-rotor, very short takeoff or landing (VSTOL) fixed wing aircraft, and fixed wing. Of these groups, the compound helicopter and the tilt-rotor were felt to provide the best solution to the requirements. VSTOL aircraft were judged to be a lesser choice because of the powerplant requirements required for operation. Helicopters and fixed wing aircraft were judged to be poor choices because the operating speeds of helicopters were too slow to be effective, and fixed wing aircraft were too large and complicated for shipboard use.

After these initial design options were investigated, two additional concepts were introduced which had the

possibility of increasing previous system capabilities. The first was Sikorsky's reverse velocity rotor (RVR), which had the potential to significantly increase the operating speeds of helicopters. The second was Lockheed-Martin's thrust-vectored lift fan, which had the potential to provide a powerplant capable of operating a large VSTOL aircraft.

The evaluation is therefore reduced to the Quad Tiltrotor, the Reverse Velocity Rotor Compound Helicopter, and the Joint Strike Fighter Lifting Fan Concept. It is believed that these three configurations offer the best attributes to meet or exceed stated requirements.

1.2.1 Quad Tiltrotor

The size of our QTR, based on the C-130 fuselage and rotor diameters of 20ft, is about 105ft long, with a rear wingspan of 70ft and a front wingspan of 55ft. The QTR can be accommodated by a CVN, although its large presence would interfere with flight operations and access to the catapults. The QTR can also be accommodated by an LHA or an LHD, but would not be able to park adjacent to the tower, which would complicate loading and unloading of equipment.

As with the V-22, the QTR has potential for high-speed flight: a speed of 245kts was used for maximum range calculations, but it could certainly dash faster. Using data from Bell (including estimates of SFC and prop efficiency), maximum range was calculated using Breuget's Range Equation and differing amounts of fuel. With 42.5k lbs available for fuel/payload, our QTR would only have 5k lbs for fuel to meet the payload requirement, resulting in

a range of about 180nm (89nm radius of action). On the other hand, satisfying the range requirement of 600nm (300nm radius of action), the payload capability is 27.5k lbs.

1.2.2 Reverse Velocity Rotor Compound Helicopter

The reverse velocity rotor (RVR) is a new concept in the helicopter community. Its goal is to increase the operating advance ratio of the rotor. This corresponds to high forward flight speeds in excess of 200 knots. Sikorsky has pioneered this idea and conducted computer simulations and some preliminary tests to validate their predictions.

Most helicopters cannot fly at high advance ratios because of the loss of lift on the retreating side of the rotor. The RVR has a unique airfoil shape that allows it to create lift, regardless of the direction of flow.

In addition to the airfoil, some other components are needed to integrate the RVR concept into an airframe. The most important of these is an auxiliary source of propulsion. At high flight speeds, the rotational velocity of the rotor will be slowed down through the use of a variable-speed transmission. This is done in order to reduce rotor losses caused by supersonic flow regions at the blade tips.

Many advantages are obtained if this RVR design is then made into a compound helicopter. These advantages include a reduction in gross weight due to increased performance. This savings in weight comes from smaller engines and less required fuel. This weight can then be

added back onto the airframe in terms of payload and fuel, helping to meet the design requirements.

Sikorsky is currently conducting extensive research and development on the RVR. The RVR has the benefit of high speed, but the disadvantage of not being a proven technology. It is clear that RVR is a potential solution to the vertical heavy-lift problem.

1.2.3 Joint Strike Fighter Lifting Fan

The JSF program has provided the group with another, more radical approach to a heavy lift aircraft in the form of its groundbreaking powerplant. Prior to the JSF program, two methods were used to extract power from turbine type engines. Conventional jet aircraft make use of turbofans. Turbofans provide cruise thrust by exhausting gases through a nozzle. However, turbofans produce no shaft power. Conversely, a turboshaft provides shaft power, but no cruise thrust.

The power plant of the Marine Corps version of the JSF is a hybrid of the two existing methods of using turbine power. In forward flight, the engine functions as a conventional turbofan and produces forty thousand pounds of thrust. In hover, the engine uses a shaft to provide power to a lift fan in the forward fuselage. Additionally, the exhaust nozzle of the engine swivels down through 90°. The thrust from the lift fan coupled with the thrust from the exhaust nozzle is sufficient to vertically lift the JSF.

The thrust required for vertical lift is almost equally distributed between the lift fan and the exhaust

nozzle. The remaining thrust comes from jets found in the wings. These small jets produce less than ten percent of the lifting thrust and are primarily responsible for roll control of the aircraft in hover.

The JSF's single engine produces 25,000 hp for the lifting fan. In comparison, both the QTR and the Compound Helicopter require 4 engines to produce comparable amounts of thrust. The primary limitation to the amount of thrust produced by the JSF's lifting fan is not the powerplant, but instead the size of the lifting fans. The small fuselage of the JSF limited the size of the lifting fan used. On an aircraft sized to fit the heavy lift requirements, the lift fan could easily be enlarged to produce more thrust. Additionally, a larger platform could more easily support both multiple lift fans and engines.

Table 1.2.1: Competing Design Concepts

Potential Design Configurations
Quad Tilt-Rotor
RVR Compound Helicopter
Joint Strike Fighter Lifting Fan

1.3 DESIGN SELECTION

Safety, performance, payload, range, maintenance, and cost were chosen as the critical elements of the design team's decision matrix. Table 1.3.1 provides an listing of the critical elements and their respective subsets.

Table 1.3.1: Design Selection Process

	Decision Matrix Critical Elements
Safety	Percieved Safety Autorotational/Glide Capability Crashworthiness/Survivability All weather capability
Payload	Ability to transport maximum cargo weight 300 nm Ability to HOGE at 4,000 ft, 95 degrees F with max cargo Ability to load and unload cargo rapidly
Performance	Cruise Speed Hover Performance Range Rate of Climb/Rate of Descent Maneuverability Flexibility
Reliability/ Maintenance	Reliability Maintainability Parts/Supplies
Cost	Initial Operating Cost Direct Operating Cost

An overview of each of these elements provides insight into the configuration selection.

1.3.1 Safety

Safety of the aircraft is paramount. The design must be crashworthy and survivable throughout the entire flight spectrum. The aircraft must be able to promote 'perceived safety' through its appearance and the behavior of similar looking historical aircraft. All weather capability must extend from the extremes of violent winters to hot-humid summer conditions. Of course, engine inoperative performance must be critiqued, with heavy emphasis on auto-rotational and glide capability.

1.3.2 Payload

For this aircraft to be successful the maximum cargo load must be transported regardless of environmental conditions. This is analogous to customer satisfaction. To ensure the loads are delivered in timely manners, the aircraft must offer unrestricted onload and offload capability.

1.3.3 Performance

The aircraft must fly two 300 nautical mile legs with adequate fuel reserves, perform maneuvers typical of a ship based assault helicopter, and offer cruise flight performance similar to a medium sized fixed wing cargo aircraft.

1.3.4 Reliability/Maintenance

The availability of the aircraft to perform this mission is critical. Short term and long term reliability and maintainability, ranging from availability/commonality of parts to the effects of vibrations on the airframe structure must all be considered in the candidate concepts.

1.3.5 Cost

Initial acquisition cost of the aircraft was not specifically identified in the requirements document but it is an important requirement. Both cost of procurement and fielding schedule, as a cost consideration, were evaluated. Fleet size was estimated to be between 90-100 aircraft.

Table 1.3.2: Preliminary Design Assessment Summary

Assessment Summary					
	Safety	Payload	Performance	Reliability / Maintenance	Cost
Quad Tilt-Rotor	⇔	↓	↑	⇔	⇔
RVR Compound	↑	↑	⇔	↑	⇔
Join Strike Fighter Lifting Fan	⇔	↑	↑	⇔	⇔
Legend: ↓ **Favorable;** ↑ **Unfavorable;** ⇔ **Medium**					

1.4 OPTIMUM CONFIGURATION

Table 1-2 clearly shows the RVR Compound as the leading design configuration with the Joint Strike Fighter Lifting Fan being the second most favorable design configuration.

Although the RVR Compound's cruising performance may not be as good as the other two configurations the target cruise speed of 205-210 knots is well within the ideal airspeed range for the specified missions. The RVR Compound's traditional compound helicopter design configuration with auxiliary propulsion bridges the gap between conventional designs and higher airspeeds, providing the optimum configuration. The compound configuration allows a substantial amount of the lift to be transferred to the more efficient wing at higher airspeeds and the RVR technology allows the rotor system to be slowed at higher airspeeds without incurring unwanted aerodynamic effects. The auxiliary propulsion provides all forward thrust at higher speeds, thus allowing the rotor tip path plane to be set to one degree, significantly reducing rotor drag.

Although nothing on the scale of the RVR Compound has ever been manufactured; *Cheyenne* flight testing clearly demonstrated that a compound helicopter with auxiliary propulsion is a very agile and capable aircraft configuration.

1.5 SUMMARY

In summary, the design team concluded that the RVR compound helicopter with auxiliary propulsion provided the optimum performance and payload combination without sacrificing safety, maintainability, and cost. The proposed aircraft was designated the CH-83 *Condor* and represents a twelve week evolution of what the design team considers the best candidate to fulfill the requirements for the Heavy Lift Rotorcraft.

2. GENERAL CONFIGURATION

2.1 LAYOUT

Figures 2.1.1 through 2.1.3 (on Page A) show's the *Condor's* basic features: a 8-blade rotor, 2 engines mounted on the fuselage and 2 engines mounted on the compound wings, 6 bladed auxiliary propellers, a conventional 6-blade anti-torque tail rotor mounted on a vertical pylon which acts as a rudder in cruise flight, and an aft cargo ramp for loading and unloading. The following sections describe in more detail the specific features and considerations used throughout the design evolution of *Condor*. This section briefly discusses several of the aircraft's systems. Detailed descriptions of structures, engines, rotors, and the compound are offered in later sections.

2.1.1 Fuselage

The fuselage includes a cockpit module, center section, and aft section. Each section is comprised primarily of composite materials using semi-monocoque construction. A detailed description of the *Condor's* structure is given in Section 3.

The cockpit module contains seats for the two pilots, installation space for the avionics in the nose bay, and the forward landing gear. A small staircase will lead to the flight deck. A jump seat is included in the cockpit to allow an evaluator or safety pilot to accompany the crew during missions. At the base of the staircase will be the Flight Engineer and Load Master stations.

The center section includes the cargo compartment, the sponsons, the wing assembly (with auxiliary propulsion), the main landing gear, the loading ramp, and the main transmission and fuselage mounted engine fairing. The sponsons house the port and starboard fuel tanks and the main landing gear.

The aft section includes the anti-torque rotor system and the horizontal and vertical tail assemblies.

2.1.2 Flight Controls

Using an in service year of 2010, it is projected that the aircraft will be fully fly-by-wire, which allows for cockpit control inputs to be digitally conditioned and mixed prior to input to the control actuators. The actuators are located adjacent to the main transmission, in the vertical pylon, in the auxiliary propulsion gearboxes, and in the wing and tail control surfaces. Two sets of flight controls are provided, allowing either pilot to command the aircraft. As with existing helicopter designs, some non-flight switches, buttons, and levers will be available from only one side of the cockpit, since redundancy is not required. All flight controls are augmented using Digital Automatic Stabilization Equipment (DASE).

2.1.3 Avionics

The *Condor's* avionics suite will offer ease of use, high speed processors, modular design, and easy upgradeability. The following sections present the top-

level avionics architecture selected for this aircraft. Critical Components of the system include:

2.1.3.1 Flight Control Computer/Mission Computer

Dual redundant flight control computers will provide the complete control of the flight control and avionics system. Commercial off-the-shelf (COTS) systems will be procured at the time of manufacture. The Flight Control Computer will use control laws established during wind tunnel experiments, full scale testing, and developmental test flights to manage aerodynamic properties of the aircraft. Of particular interest will be the Flight Control Computer's ability to implement 1P plus 2P control of the rotor system and the ability to warn to pilots of impending Vortex Ring State conditions. The Flight Control Computer will also automatically vary the speed of the rotor system while the aircraft increases to cruise speed (full use of RVR technology).

The mission computer will greatly reduce the crew workload during flight operations in hostile environments. The crew will be able to plan nearly all aspects of a mission using a desktop workstation and then transfer the information using a modified memory card to the *Condor*. After successful data transfer the flight route, threat assessment, weather forecast, radio frequencies, expected cargo configurations, and performance planning will all be accessible from the flight deck.

2.1.3.2 Controls and Displays

The control and display system relies on the current development of flat panel display technology. Four color flat panel displays will present all data to the flight crew for navigation, communication, sensor systems, and air vehicle monitoring. The Flight Engineer and the Loadmaster will also have one display each to provide relevant data. A series of pre-configured data displays will be available to each crew member through selectable hierarchy type menus and Variable Action Buttons (VABs) located around the edges of each display. All flight critical displays will be standardized but non-critical displays such as fuel management can be customized to meet crew preferences or mission requirements. A small cluster of analog instruments displaying essential flight, powerplant, and communications information will be available in the event of flight computer failure. All displays and flight instruments will be Night Vision Google (NVG) compatible.

2.1.3.3 Dynamic Health Usage and Monitoring System (DHUMS)

The *Condor* will utilize a fully integrated DHUMS for all critical dynamic components (engines, main transmission, tail rotor, auxiliary propulsion, transmissions, etc.). The embedded sensors will monitor critical aircraft parameters and create data logs containing time histories of operation. Main rotor, tail rotor, and propeller blade track and balance vibrations

will be monitored and recorded continuously. Data will be shared with the Flight Control Computer to ensure proper inputs are provided to each system. This data integration will permit the use of a pilot cueing system that will increase control resistance (through the use of micro-actuators attached to the flight controls) as the pilot approaches or enters into power/temperature/time-limit areas. Maintenance personnel will be able to access the information directly from the Flight Engineer station or download the data for further analysis. The DHUMS database will contain all pertinent electronic technical manuals and parts listings. This system will all but eliminate the traditional paper logbook.

2.1.3.4 Navigation

The navigation system will be a dual Embedded Global Positioning System/Inertial Navigation System (EGI). This system was developed for the military and has proven itself by providing highly accurate navigation and attitude information. The inertial navigation components of this system will provide high fidelity data for the Stability Control Augmentation System. The system is highly reliable in all modes of flight. Standard VOR/DME capabilities are included in the avionics configuration to solidify the *Condor's* IFR capabilities.

2.1.3.5 Communications

All standard UHF/VHF communications requirements will be meet. Additionally the communications system will be able to us HF and data links to satisfy emerging

communication requirements. Fused communication data will be displayed with critical weather and terrain avoidance data.

2.1.4 Fuel System

The fuel system provides fuel to all four engines and the APU. Fuel is contained in two self-sealing, crash resistant fuel cells located in the sponsons. Each cell contains 1200 gallons. Typically the port cell will be used to supply fuel to the APU and port engines and the starboard cell will supply fuel to the starboard engines. Fuel can be transferred between both cells using transfer pumps. In case of fuel system damage or partial failure cross feed and alternate feed valves all each engine to select fuel from any cell. Fuel management can also be accomplished automatically via the Mission Computer to ensure favorable lateral CG location. Additionally auxiliary fuel tanks may be mounted inside the cargo compartment for ferry flights. The *Condor* also possesses the capability to conduct aerial refueling.

2.1.5 Aircraft Subsystems

Aircraft subsystems are comprised of the Auxiliary Power Unit (APU), the hydraulic system, the electrical system, and the pressurized air system.

2.1.5.1 APU

The Auxiliary Power Unit (APU) powers all subsystems through the main transmission prior to rotor

engagement and provides high pressure bleed air for engine starting and cabin environmental control. APU starting is accomplished using pressurized air provided by the hydraulic accumulator. The high pressure air is released either by cockpit control or by using a manual switch located on the APU (for maintenance personnel only). After rotor engagement (100% rpm) an overriding clutch assembly unloads the APU driveshaft and the crew secures the APU.

2.1.5.2 Hydraulic System

The *Condor* has four hydraulic pumps. Each auxiliary propulsion engine has its own pump and two pumps are mounted on the transmission accessory gearbox. The wing mounted hydraulic pumps are used to power flight control surfaces, auxiliary propulsion propeller pitch control actuators, and utility systems while the transmission mounted pumps power the main rotor and tail rotor actuators (flight control systems). Utility subsystems include the landing gear actuators, main landing gear brakes, the cargo ramp, and the APU accumulator. All hydraulic pumps deliver 3000 psi. These four systems have the capability to cross over and provide hydraulic power to the other systems if required.

2.1.5.3 Electrical System

All the aircraft electrical power requirements are supplied by two AC generators, two transformer/rectifiers (T/Rs), for DC power, and in the case of a complete failure, three 24 volt batteries will supply flight critical systems. The generators are mounted

on and driven by the main transmission accessory gearbox. Each generator and its associated components comprise an independent ac generating system that supply about one half of the total electrical requirements to the ac buses.

2.1.5.4 Pressurized Air System (PAS)

The PAS cleans, pressurizes, regulates, and distributes air to the engine air turbine starters, fuel boost pumps, fuel transfer pumps, and other pneumatic subsystems. The primary source for the PAS is the port fuselage mounted engine and the secondary source is the starboard fuselage mounted engine.

2.1.6 Landing Gear

The *Condor* is equipped with tricycle style landing gear. The configuration is very similar to that of a typical C-130. The resulting footprint of the aircraft makes it compatible with existing amphibious assault ships. All three sets of landing gear are fully retractable and can withstand a static load of 150,000 lbs. When retracted the landing gear wells close with flush mounted, electrically held, spring actuated doors. While taxiing the aircraft is fully steerable using a hand wheel located in the left pilot station. If necessary, the nose gear can be electrically decoupled from the hand wheel and the aircraft can be turned using the anti-torque pedals.

In the event of an emergency where electric and/or hydraulic power is lost the doors will automatically spring to the open position and the landing gear may be blown down using a one-way nitrogen blow down system. After blow-down,

the landing gear may be raised if electrical and hydraulic power is restored, but the blow down system can not be used until recharged by maintenance personnel.

The landing gear is comprised of approximately 25% aluminum (wheels), 10% composites (brakes), and 65% titanium (struts, trolley arms, axles). During a severe landing the titanium struts are designed to deform to absorb maximum energy without detaching from their bulkhead connection points. In the most extreme circumstances shear rings inside each strut are sheared and a rupture disk burst causing a controlled collapse of the strut.

2.1.7 Aircraft Survivability Equipment (ASE)

Since the *Condor* is purpose designed to operate in hostile environments an ASE suite is included in the overall design. A next generation radar warning receiver (ALR-69 type), IR Jammer (ALQ-144 type), Chaff/Flare dispenser (ALE-40 type), and an advanced Electronic Counter Measures Pod (ALQ-131 type) are installed on the aircraft. An ASE control subroutine in the Flight Control Computer fuses all sensor data an can either cue the pilot with recommended actions or work automatically to decrease overall aircraft suspectability. Survivability is discussed in greater detail in Section 11.

2.1.8 Cargo Management System

The *Condor's* Loadmaster will operate a state of the art Cargo Management System (CMS) which will allow him to calculate weight, center of gravity, and optimum load configurations. The CMS will house an extensive database of

expected loads, pallet arrangements, vehicles, and technical manuals. The CMS incorporates motorized rollers in the cargo floor to move pallets and an integrated winch to assist in pulling wheeled vehicles or trailers onboard. Loading will be able to occur with engines running or stopped. Load cells located within each landing gear trolley assembly will allow the crew to 'weigh' the aircraft with a high degree of fidelity. Three closed circuit movable (elevation, azimuth, and zoom) video cameras will allow the Loadmaster to survey the cargo from nearly every angle. All data and video can be easily sent to the flight deck for pilot information. Overhead lighting will be NVG compatible.

2.2 INITIAL SIZING

Amongst all the design requirements specified for this project, three key requirements were selected as the primary target parameters for performance calculations, namely range, speed and payload. The performance calculation was broadly classified into five main categories, namely, rotor sizing, compound wing sizing, weight sizing, main engine and tail rotor/auxiliary propulsion sizing as shown in figure 1. The five categories calculation were closely coupled and inter-related. Changes in any one of the categories of calculation would affect the other categories' calculation. Hence, the performance calculation of the *Condor* was very much an iterative process.

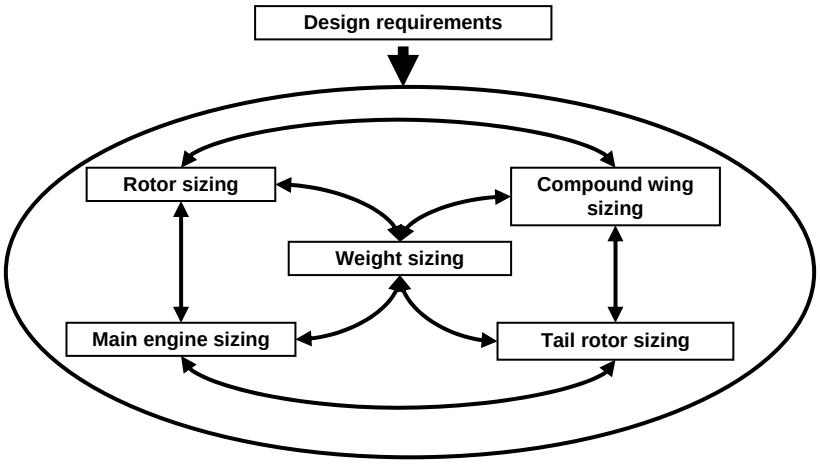

Figure 2.2.1: Broad categories of performance calculation for the design helicopter

A Microsoft Excel spreadsheet was programmed to calculate the performance calculation. The optimization module within Excel was utilized to achieve the most optimum set of parameters.

2.2.1 Key Design Target Parameters

The critical design requirements for this project were for the aircraft to have a minimum of 300 nm radius of action and to carry a minimum of 37,500 lbs of payload. The aircraft was also desired to cruise at speeds in excess of 200 knots in order to minimize transit time. In addition, the system was allowed to have, as a maximum, a spot factor no larger than twice that of the CH-53E (threshold), but preferable a spot factor no more than 1.5 times that of the CH-53E. This spot factor requirement applied to both spread and folded configurations.

As mentioned earlier, three key target design parameters were selected to be the main driver for the performance calculation. Range, speed and payload were the key target design parameters. A range of 600nm (since a

radius of 300nm is required), speed in excess of 200kts and a payload of 37,500lbs were the figures used as target parameters in the performance calculation.

2.2.2 Weight Sizing

The performance calculation began with the weight sizing. Gross weight, G.W. and fuel weight, W_f were estimated first. Payload, $W_{payload}$ was required to be 37,500lbs since it was a key target parameter. W_f was initially estimated from the following equation:

$$W_f = \text{sfc} \times HP_{\text{estimated installed}} \times \text{mission time} \qquad (2.2.1)$$

Useful load was computed to estimate the Gross weight. Useful load is defined as

$$Load_{useful} = \text{crew weight} + \text{payload} + \text{fuel weight} \qquad (2.2.2)$$

Using Figure 2.2.2 and the value of $Load_{useful}$, GW was estimated as follows:

$$GW = \frac{Load_{useful}}{\frac{Load_{useful}}{GW}} \qquad (2.2.3)$$

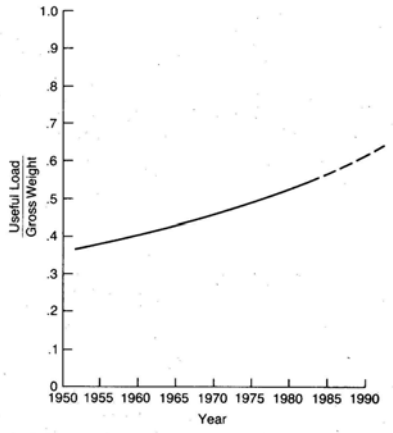

Figure 2.2.2: Historic trend of ratio of useful load to gross weight

2.2.3 Rotor Sizing

With the GW estimated, the thrust required for the rotor was assumed to be 20% of GW in forward flight and 100% of GW in hover flight. Based on existing CH-53E and MI-26 helicopters, the number of blades, b, blade radius, R and blade chord, c, were estimated. Based on the estimated R, the rotor's rotational speed, RPM was selected such that the tip speed do not exceed 0.9 Mach. With b, R, c and RPM estimated, the following parameters were calculated as follows:

Disc area, $A = \pi R^2$ (2.2.4)

Solidity, $\sigma = \frac{bc}{\pi R}$ (2.2.5)

Disc loading, $DL = \frac{T}{A}$ (2.2.6)

Induced velocity, $V_i = \sqrt{\frac{DL}{2\rho}}$ (2.2.7)

Blade tip speed at ψ=0, $V_{tip,0} = \Omega R$ (2.2.8)

Blade tip speed at ψ=90, advancing blade,

$V_{tip,90} = \Omega R + V_{fwd}$ (2.2.9)

Blade tip speed at ψ=0 $V_{tip,180} = \Omega R$ (2.2.10)

Blade tip speed at ψ=0, retreating blade,

$V_{tip,270} = \Omega R - V_{fwd}$ (2.2.11)

Advance ratio, $\mu = \frac{V_{fwd}}{\Omega R}$ (2.2.12)

Thrust coefficient, $C_T = \dfrac{T}{\rho A(\Omega R)^2}$ (2.2.13)

From Equations (2.2.5) and (2.2.13), the value of $\dfrac{C_T}{\sigma}$ was obtained and used in figure 3 to obtain $\dfrac{C_Q}{\sigma}$. The torque, Q was then calculated from the following equation:

Torque coefficient, $C_Q = \dfrac{Q}{\rho A(\Omega R)^2 R}$ (2.2.14)

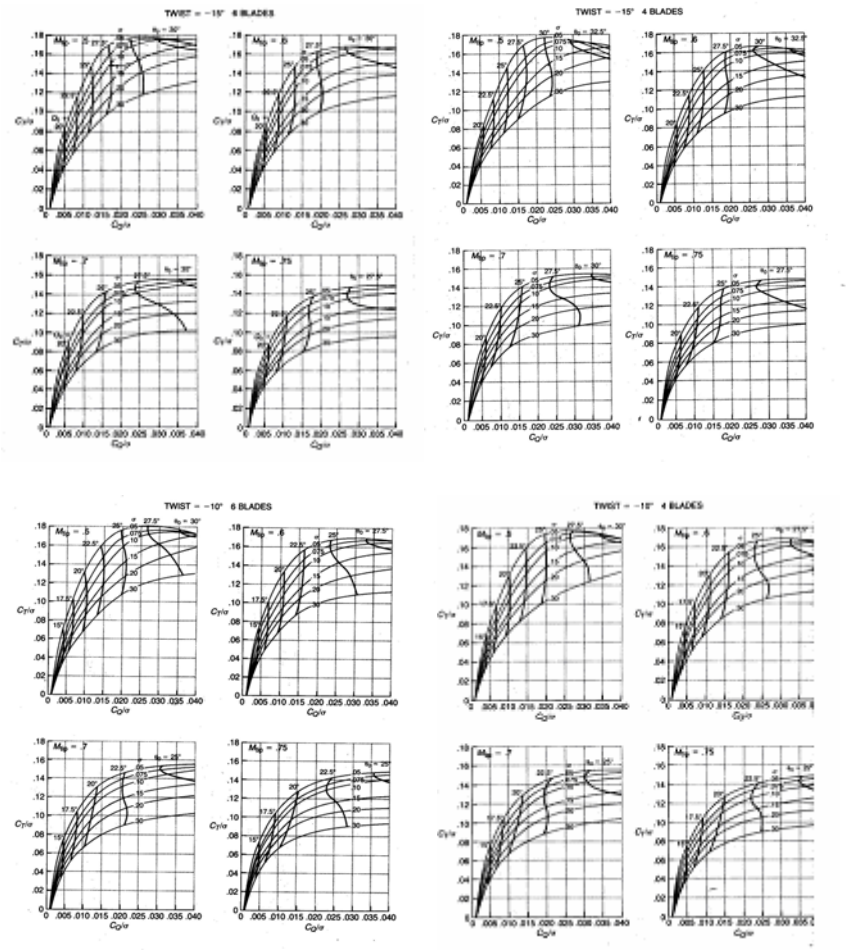

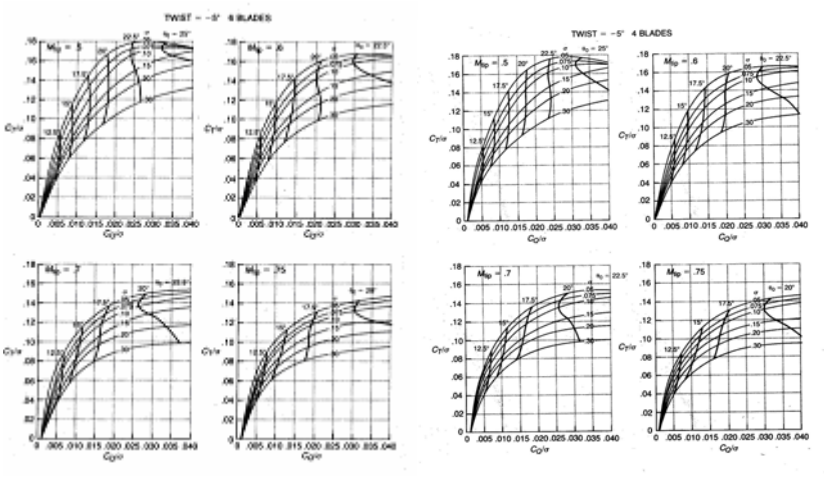

Figure 2.2.3: Historical experimental data of $\frac{C_T}{\sigma}$ variation with $\frac{C_Q}{\sigma}$ for different number of blades and angle of twist.

2.2.4 Tail Rotor Sizing

The tail rotor sizing began with the value of torque, Q obtained from Equation (2.2.14). This was the value of the anti-torque that the tail rotor has to provide. With the preliminary dimensions of the aircraft estimated based on the C130 fuselage body, the moment arm, $L_{moment\ arm}$ was estimated and used to compute the required thrust by the tail rotor, $T_{tailrotor}$, as:

$$T_{tailrotor}\ L_{moment\ arm} = Q \qquad (2.2.15)$$

Similar to the main rotor, the thrust coefficient of tail rotor, $C_{T\text{-}tail\ rotor}$, was computed as shown in Equation (2.2.16) with estimated figures of RPM of tail rotor, $\Omega_{tail\ rotor}$ and radius, $R_{tail\ rotor}$. The $\Omega_{tailrotor}$ and $R_{tailrotor}$ values were estimated based on historical design data and approximately relative size from the main rotor.

$$C_{T-tailrotor} = \frac{T_{tailrotor}}{\rho A_{tailrotor}(\Omega_{tailrotor} R_{tailrotor})^2} \qquad (2.2.16)$$

The solidity of the tail-rotor, $\sigma_{tailrotor}$ was also estimated based on typical helicopter tail rotor values so that $\frac{C_{T-tailrotor}}{\sigma_{tailrotor}}$ can be computed for use in Figure 2.2.4 to obtain $\frac{C_{Q-tailrotor}}{\sigma_{tailrotor}}$.

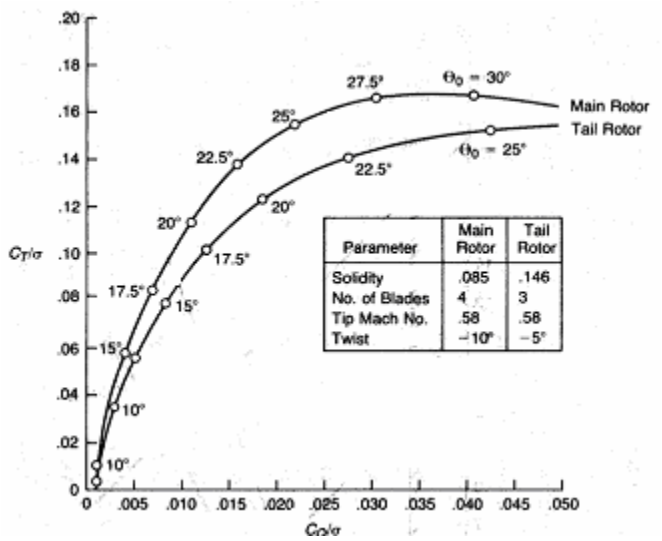

Figure 2.2.4: $\frac{C_{T-tailrotor}}{\sigma_{tailrotor}}$ variation with $\frac{C_{Q-tailrotor}}{\sigma_{tailrotor}}$

The torque of the tail rotor was hence computed similarly to the main rotor as:

Tail rotor torque coefficient,

$$C_{Q-tailrotor} = \frac{Q_{tailrotor}}{\rho A_{tailrotor}(\Omega_{tailrotor} R_{tailrotor})^2 R_{tailrotor}} \qquad (2.2.17)$$

Power required for the tail rotor was calculated as:

$$P_{tailrotor} = \frac{Q_{tailrotor}\Omega_{tailrotor}}{550} \qquad (2.2.18)$$

To account for Tail Rotor-Fin interference in hover the following equations were used:

$$T_{Tgross} = \frac{T_{Treq}}{1 - F/T} \qquad (2.2.19)$$

$$hp_T = \left(1 - \frac{F/T}{2}\right)(h.p.T_{Tgross}) \qquad (2.2.20)$$

The interference ratio (F/T), from page 286 of Prouty's textbook, was found to be 5%.

2.2.5 Engine Sizing

With the value of torque Q, obtained for the main rotor, the power required for the main rotor to hover was obtained as follows:

Power required for rotor to hover, $P_{hover} = \frac{Q\Omega}{550}$ (2.2.21)

The total power required to size the engine system not only include P_{hover} but power required for accessories, $P_{accessories}$, power required vertical climb, $P_{vert\ climb}$, power required for tail rotor, $P_{tail\ rotor}$ and reserve power, $P_{reserved}$. Therefore, the total power required, $P_{required}$, is computed as follows:

$P_{required} = P_{hover} + P_{accessories} + P_{vert\ climb} + P_{tailrotor} + P_{reserved}$ (2.2.22)

$P_{accessories}$ was estimated to be 3% of P_{hover} based on typical historical helicopter design data. Similarly, $P_{reserved}$ was estimated to be 5% of (P_{hover} + $P_{accessories}$ + $P_{vert\ climb}$ + $P_{tailrotor}$). $P_{vert\ climb}$ was computed as follows:

$$P_{vertclimb} = \Delta P_{climb} = \frac{GW}{550}[\frac{V_c}{2} + \sqrt{\{(\frac{V_c}{2})^2 + V_{i,hover}{}^2\}} - V_{i,hover}] \qquad (2.2.23)$$

2.2.6 Compound Wing Sizing

With the GW estimated, the lift required for the compound wing was assumed to be 80% of GW in forward flight and 0% of GW in hover flight. Therefore, the compound wing sizing is for forward cruise performance. A lift coefficient, C_L of 0.6 was assumed. This was a reasonable assumption since most airfoils are capable of producing a C_L of 0.6 at a cruise speed in excess of 200 knots. The wing-span, b and chord length, c of the wing as estimated based on the C130's wing. Using the following equations, the planform area, S and the aspect ratio, AR of the wing was computed:

$$L = \frac{1}{2}\rho V^2 C_L S \qquad (2.2.24)$$

$$AR = \frac{b^2}{S} \qquad (2.2.25)$$

2.2.7 Summary of Initial Sizing

Equations 2.2.1 through 2.2.25 allowed the initial sizing to be carried out. This was done using Microsoft Excel® and utilizing the Optimization Module in the software to achieve the best possible results. Table 2.2.1 summarizes the results.

Table 2.2.1: Summary of initial sizing values

Parameters	Computed based on altitude 4000ft, temperature 95°F conditions
Weight sizing	
W_{empty} (lbs)	64513.6
$W_{payload}$ (lbs)	37500.0
W_f (lbs)	15283.8
GW (lbs)	117297.4
Rotor sizing	
R (ft)	55.3
c (ft)	4.1
B	8
Ω(RPM)	105.3
A (ft^2)	9607.3
Σ	0.190
DL (psf)	12.2
V_i (fps)	56.4
$\frac{C_T}{\sigma}$	0.0900
$\frac{C_Q}{\sigma}$	0.0120
Q (ft-lb)	864873
Tail Rotor sizing	
$R_{tailrotor}$ (ft)	12.5
$c_{tailrotor}$ (ft)	1.31
$b_{tailrotor}$	6
$\Omega_{tailrotor}$ (RPM)	600
$\sigma_{tailrotor}$	0.2
$\frac{C_{T_{tailrotor}}}{\sigma_{tailrotor}}$	0.11
$\frac{C_{Q_{tailrotor}}}{\sigma_{tailrotor}}$	0.02
$Q_{tailrotor}$ (ft-lb)	24925

Parameters	Computed based on altitude 4000ft, temperature 95°F conditions
Engine sizing	
P_{hover} (HP)	17340
$P_{anti-torque}$ (HP)	2776
$P_{accessories}$ (HP)	520
$P_{vert\ climb}$ (HP)	360.70
$P_{reserve}$ (HP)	1053
$P_{required}$ (HP)	22047
Compound wing sizing	
C_L	0.60
b (ft)	96.00
c (ft)	13.01
S (ft^2)	1248.71
AR	7.38

2.3 CARGO COMPARTMENT/ARRANGEMENT

The size of the cargo compartment was based on the required payloads specified in the ORD. It was stated that the airframe needed to be capable of transporting Light Armored Vehicles (LAV), Heavy Expandable Mobile Ammunition Trailers (HEMAT), and Medium Tactical Vehicle Replacements (MTVR). The weight and sizes of these automobiles are located in Table 2.3.1. A slight margin was added to these dimensions to provide adequate clearance and moving space. Specifically, 14-inch wide aisles were provided on either side of the widest load, and 12 inches of clearance was allowed for both the length and height dimensions. The final cargo space dimensions can be seen in Table 2.3.2.

Table 2.3.1: Weight and sizes of vehicles

	LAV	**HEMAT**	**MTVR**
Length(in)	251.6	307	314.9
Height(in)	106	70	125
Width(in)	98.4	98.4	98.4
Weight (lbs)	28200	32850	28000

Table 2.3.2: Final cargo space dimensions

REQUIRED CARGO SPACE		
	inches	**Feet**
Length	326.9	27.24
Height	137	11.42
Width	126.4	10.53
Weight (lbs)	32850	

2.3.1 Load Cases

A total of seven load cases were analyzed for use with the CH-83 *Condor*. Three cases were explicitly outlined in the RFP and the rest were based on standard military heavy-lift transport missions. The seven load scenarios studied were:

Troop transport

Air Ambulance

Pallet Loading

LAV

HEMAT

MTVR

HUMVEE

All handling and securing of equipment located inside the cargo bay is identical to the technology incorporated in the C-17. These include floor roller tracks, hooks for ropes and chains, and standard pallet securing setups. A summary of each load configuration capacity can be seen in Table 2.3.3. The effects of the cargo on the overall aircraft CG can be found in Chapter 10.

Table 2.3.3: Summary of each load configuration capacity

LOAD CAPACITY FOR DIFFERENT CONFIGURATIONS	
Load Case	**Qty**
Troop Transport	124 troops
Air Ambulance	63 litters
Pallet Loading	6 pallets
LAV	1
HEMAT	1
MTVR	1
HUMVEE	3

2.3.1.1 Troop Transport

For the troop transport mission the first assumption made was to classify each person aboard as a Category 2 passenger weighing 300 lbs. Category 2 is the Army standard for a soldier carrying load bearing equipment (LBE), weapon, helmet, rucksack, and organizational equipment. Given that the entire available payload was used for personnel, the CH-83 was found to have a troop capacity of 124 Category 2 soldiers. The layout of this load plan is seen in Figure 2.3.1. Each seat is assumed to be 18 inches deep by 21 inches wide, and the aisles are each 24 inches wide.

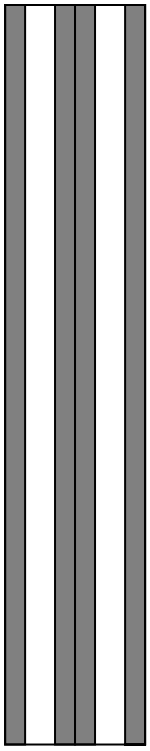

Dark Gray indicates the seating area

Figure 2.3.1: Layout of troop transport

2.3.1.2 Air Ambulance

The air ambulance mission assumed that every patient would be contained on a Stoke's stretcher. These provide the patient with maximum support and are frequently used in military applications. A picture of this stretcher can be seen in Figure 2.3.2. The weight of each stretcher is 32 lbs, and it is 84 inches long by 24 inches wide.

• Weight 31 lbs.
• Dimensions 24" x 7.25" x 84"

Figure 2.3.2: Picture of stretcher

When laying out the load configuration for this mission certain medical and logistical criteria needed to be met. For example, doctors and nurses need to have access to their patients, and stretchers are more easily stowed head to toe by those carrying them. After considering various criteria, the final load configuration was determined and can be seen in Figure 2.3.3. For this load configuration 300 lbs was accommodated for each patient and stretcher. There are seven litters per row, stacked three high, with 6 inches between stretchers. The total carrying capacity of this configuration is 63 litters.

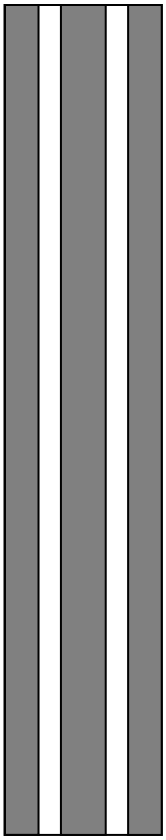

Dark Gray indicates the litter storage spaces.

Figure 2.3.3: Final load configuration for air ambulance

2.3.1.3 Pallet Loading

Each pallet has a maximum capacity of 10,000 lbs. There is room for six pallets in the cargo bay, but with fully loaded pallets this would exceed the maximum payload. There were a large number of possible pallet load configurations, so only the most practical one was selected. This is the load case of six pallets, each one weighing 6250 lbs. The dimensions of the pallet are 108 by 88 inches. It is assumed that the pallets are loaded correctly so that their CG lies at the geometric center of the pallet, and that C-17 pallet loading technology is used

to secure the pallets in place. The pallet load configuration can be seen in Figure 2.3.4.

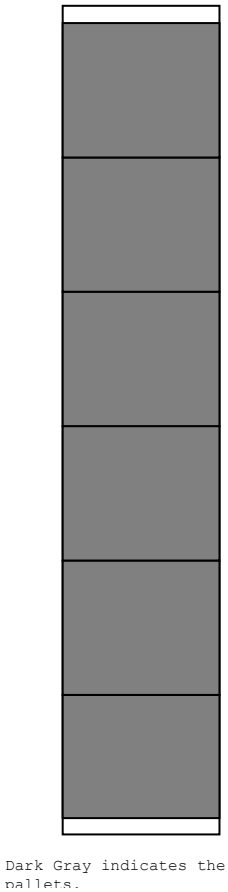

Figure 2.3.4: Final load configuration for pallet

2.3.1.4 LAV, HEMAT, MTVR

It was assumed for all three of these load cases that the vehicles would be loaded in backwards to decrease the offload time. All three vehicles could not be placed at the front of the cargo compartment because of the need to accommodate the overall CG location of the aircraft. Due to the weight of the chains and securing straps need to hold these vehicles in place, and the unavoidable wasted space needed to accommodate the overall aircraft CG, no other cargo was loaded with this configuration. The load plans

for these three vehicles can be seen in Figures 2.3.5 through 2.3.7 respectively.

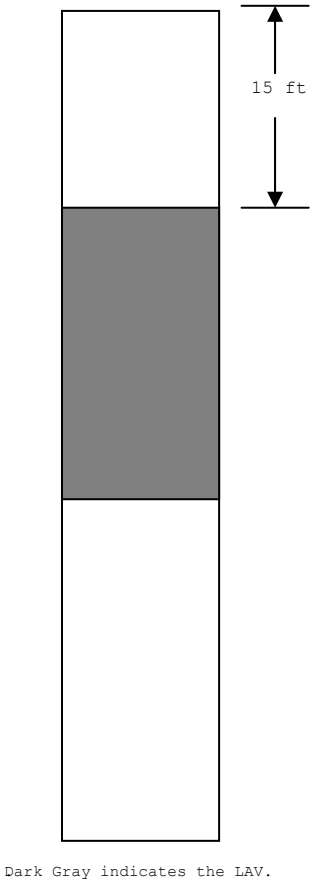

Figure 2.3.5: Final load configuration for LAV

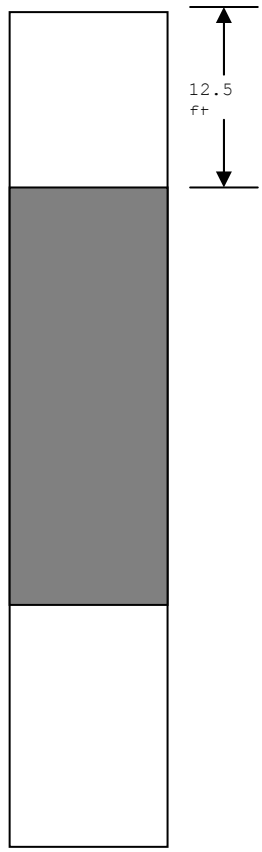

Dark Gray indicates the HEMAT.

Figure 2.3.6: Final load configuration for HEMAT

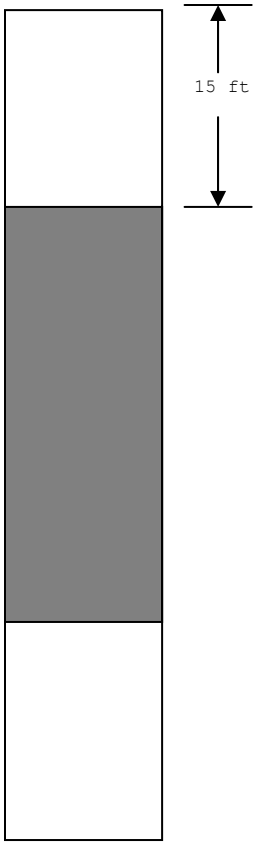

Dark Gray indicates the MTVR.

Figure 2.3.7: Final load configuration for MTVR

2.3.1.5 HUMVEE

Unlike the three previous load cases, the HUMVEE was a relatively light vehicle. It had an unloaded weight of 7000 lbs, but 1000 lbs was added to accommodate the numerous variants (e.g. machine gun mounts and ammo) as well as the securing chains and straps. The CH-83 has adequate cargo space to carry three HUMVEE's with two feet between each vehicle. The HUMVEE load configuration can be seen in Figure 2.3.8.

Dark Gray indicates the HUMVEEs.

Figure 2.3.8: HUMVEE load configuration

2.4 MAINTENANCE ACCESS AND SERVICE

The *Condor* is designed for all maintenance actions and servicing to be simple, efficient, and performed with the minimum number of tools. No support equipment (maintenance stands) is required to complete daily and scheduled maintenance actions since recessed steps and work platforms are designed into *Condor's* airframe. One eight foot ladder must be flown with the aircraft so the Flight Engineer can access the auxiliary propulsion powerplants The Flight Engineer will use a standard aviation toolkit (for Cargo

Helicopters) to complete a pre-mission inspection or between flight turnaround.

2.4.1 Exterior Access

For maintenance and repair the *Condor* has been designed for easy access to all major subsystems. Engines, hydraulics, electrical systems, the APU, and main transmission can be accessed through panels on the main fuselage fairing. At the rear of the fairing a split is cut to allow access to a catwalk between the two engines right up to the main transmission. Built in recessed steps allow access to the wing root from both sides of the fuselage. Auxiliary propulsion engines are accessible with the eight foot ladder and wide opening cowlings.

The tail pylon also offers recessed steps for easy access to the tail rotor gearbox. The upper portion of the tail pylon folds out to reveal a work stand capable of supporting the weight of two men. Access panels also allow easy inspection or maintenance of the tail rotor intermediate gearbox.

The avionics components are directly accessible in the aft cockpit and through the nose bay. An external power receptacle is located immediately aft of the port side sponson. Ground personnel interphone plugs are located on the nose landing gear and immediately inside the cargo ramp.

2.4.2 Interior Access

The cargo compartment overhead allows hinged access to inspect structural members of the wing and main transmission support. Hydraulic lines, electrical wires, the pressurized air system (PAS), and fuel lines are accessible through removable panels. Main fuel shutoff valves are located port and starboard above the sponsons and are accessible from the cargo compartment.

3. STRUCTURE

3.1 DESCRIPTION

The main structural components of the *Condor* can be seen in figure 3.1.1: a cockpit section, the main fuselage body, and a tail section leading to the horizontal and vertical tails, as well as the tail rotor. This general appearance changed quite a bit from the original design for the *Condor*. The body, in particular, evolved from what was originally a straight C-130J-30 fuselage to a much more efficient shape for the *Condor*'s mission requirements. One of the important aspects of the structural design in fulfilling those requirements was the use of composite materials.

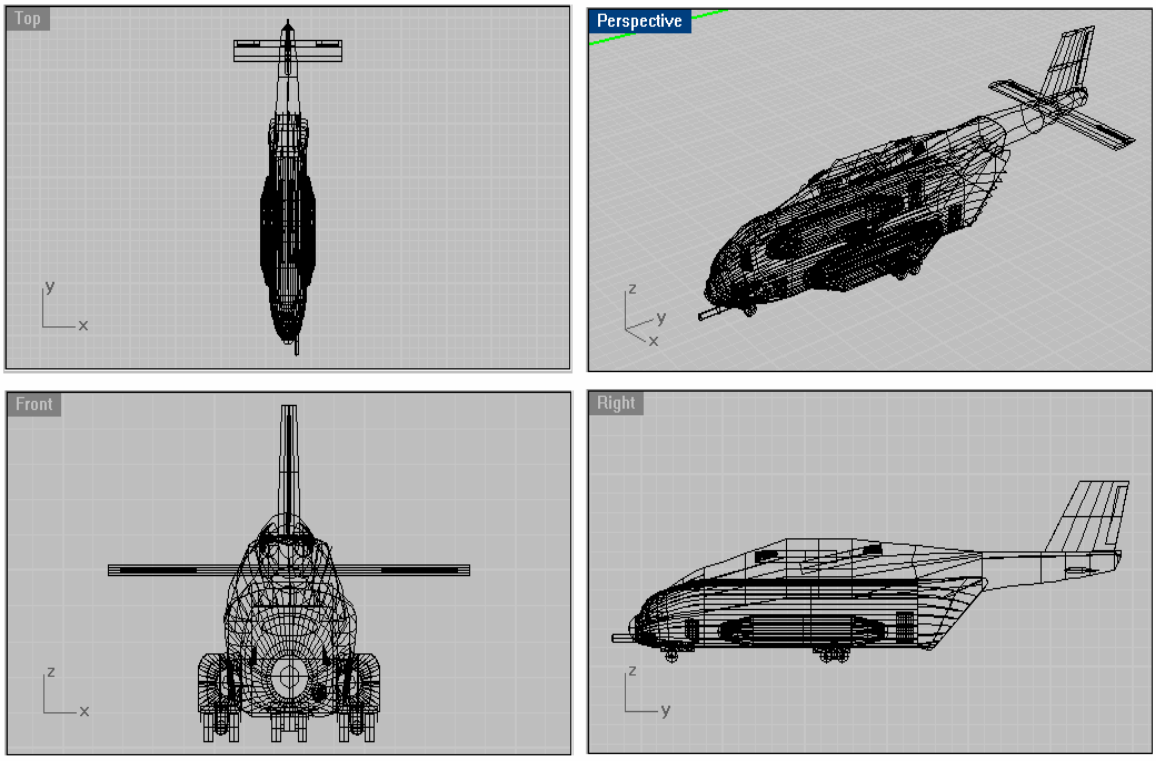

Figure 3.1.1: Structural View, Overhead

3.1.1 Composites

The goal for the structural design of the *Condor* was to reduce its empty weight by 10% through the use of at least 70% composite materials – a benchmark set by the V-22 *Osprey*. A key to achieving this goal was to incorporate composites into primary load-bearing structures, as well as the more conventional places for composites like secondary structures. The first step in composite design was selecting what material to use. This was done by looking at different matrices and fibers, and then comparing the physical and structural properties of some composite materials that are already being used in industry.

Figure 3.1.3 lists attributes of several common thermosetting resins, or matrices. This figure comes from Composite Airframe Structures by Niu, which, along with Composite Materials in Aerospace Design by Zagainov, were the primary references for composite material data. As can be seen, the chart lists resins in order of increasing heat resistance; however, for the *Condor*'s subsonic flight regime, heat resistance was not going be an issue. The important attributes for our choice of resin (keeping in mind that this composite material was to be used in primary load-bearing structures) were mechanical properties and, of course, cost. Based on this, epoxy was the best choice for a resin. Epoxy also brought the added advantage of many years of testing and development. Therefore, there would be quite an extensive database available on the properties of epoxy-based components to assistance in the detailed design process.

Characteristics	Thermosetting resins				
Property	Polyester	Epoxy	Phenolic	Bismaleimide	Polyimide
Processability	Good	Good	Fair	Good	Fair to difficult
Mechanical properties	Fair	Excellent	Fair	Good	Good
Heat resistance	180°F	200°F	350°F	350°F	500-600°F
Price range	Low — Medium	Low — Medium	Low — Medium	Low — Medium	High
Delamination resistance	Fair	Good	Good	Good	Good
Toughness	Poor	Fair — Good	Poor	Fair	Fair
Remarks	Used in secondary structures, cabin interiors, primarily with fiberglass	Most widely used, best properties for primary structions; principal resin type in current graphite production use	Used in secondary structures, primarily fiberglass good for cabin interiors for low smoke generation	Good structural properties, intermediate temperature resistant alternative to epoxy	Specialty use for high temperature application

Figure 3.1.2: Comparison of Thermoset Matrices

The next step in composite construction was selecting a fiber. Figure 3.1.3 (from Niu's text) lists attributes of several commonly used composite fibers. As is evident from the two tables, carbon/graphite is an excellent choice for primary structures, and has good tensile, compressive and shear properties. (Carbon and graphite refer to the same general material, but carbon fibers are 93-95% carbon, while graphite fibers are more than 95% carbon.) According to Niu, "The outstanding design properties of carbon/matrix composites are their high strength-to-weight and stiffness-to-weight ratios. With proper selection and placement of fibers, composites can be stronger and stiffer than equivalent steel parts at less than half the weight."

- Graphite
  Most widely used for primary structural applications; best balance of properties, cost, handleability; wide range of fiber types and properties
- Aramid (Kevlar-49)
  Uses limited by low compression strength and poor bond to resins; lighter weight and lower cost than graphite; good impact resistance
- Boron
  Very high cost, difficulty in handling have limited boron to specialty use where its combination of high strength and stiffiness is needed
- Fiberglass
  Much lower stiffness has limited use to secondary structures

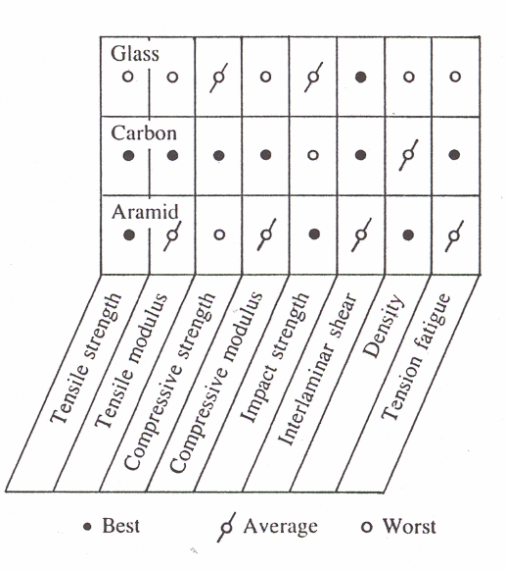

Figure 3.1.3: Comparison of Composite Fibers

Kevlar, while a good material with extremely low density, has very poor compressive properties. Since both the upper surface of the wing as well as the upper and lower surfaces of the fuselage is primarily loaded in compression, Kevlar was not a suitable choice. The chart says that boron is prohibitively expensive, which can be seen better in another table from Niu's text shown in figure 3.1.4. Obviously this eliminated boron from use in large composite structures like the body and wings, which was unfortunate because it has ***very*** good properties in tension, compression and shear. Lastly, glass-based composites have some good properties in shear and compression, but didn't have the stiffness required to make them viable load-bearing structures. They could, however, be later incorporated into secondary structures like the cabin and cargo bay interiors.

Composite Fibers	Costs per pound
Boron	>$200
Graphite	
Standard PAN based (33 × 10^6 modulus)	
1,000 TOW	$135
3,000 TOW	$ 38
6,000 TOW	$ 28
12,000 TOW	$ 24
Intermediate modulus	
12,000 TOW	$ 45
6,000 TOW	$ 85
High modulus	$650
Kevlar	$ 15-20
Fiberglass	$ 3-5
Quartz	$110

Figure 3.1.4: Cost Comparison of Composite Fibers

The next comparison was between the actual physical and structural properties of selected composite materials. This comparison was somewhat preliminary, however, because an exhaustive list of composites (which could be found in MIL-HDBK-17, "The Composite Materials Handbook") was not available. So, figure 3.1.5 lists and compares several properties of the following materials: glass/epoxy, graphite/epoxy, aramid(Kevlar)/epoxy, and boron/epoxy. The real design-driving factors were listed under "Calculated Design Parameters." Graphite/epoxy ranked first in both elastic buckling and stiffness, and also came in close second for two of the remaining three parameters. Hence, graphite/epoxy was chosen as the primary construction material for the aircraft's structure.

Composite Material Properties

		glass/epoxy	graphite/epoxy	aramid/epoxy	boron/epoxy	(units)
Material Properties:						
density	rho	0.00675	0.0057	0.0048	0.00725	lb/in^3
		1.87E-07	1.58E-07	1.33E-07	2.01E-07	kg/mm^3
modulus of elasticity	E	5500	16000	6000	19500	kg/mm^2
shear modulus	G	5500	5500	1750	575	kg/mm^2
poisson's ratio	mu	0.3	0.295	0.3	0.3	kg/mm^2
ultimate strength in...						
tension	Ftu	150	125	165	150	kg/mm^2
compression	Fcu	60	115	25	210	kg/mm^2
shear	Fsu	4	7.5	5	9	kg/mm^2
Calculated Design Parameters:						
elastic buckling	= sqrt(E)/rho	3.97E+08	8.01E+08	5.83E+08	6.95E+08	--
stiffness	= E/rho	2.94E+10	1.01E+11	4.51E+10	9.71E+10	mm
specific strength in...						
tension	= Ftu/rho	8.02E+08	7.92E+08	1.24E+09	7.47E+08	mm
compression	= Fcu/rho	3.21E+08	7.28E+08	1.88E+08	1.05E+09	mm
shear	= Fsu/rho	8.89E+03	2.02E+04	5.21E+03	2.90E+04	mm

Figure 3.1.5: General Properties for Selected Composites

The only remaining consideration was to decide on a ply orientation for the multiple layers of graphite/epoxy that would be used for different sections of the structure. (Anywhere from 4-8 layers for control surfaces up to 20 layers for the wing.) Because composite materials have virtually no strength across the direction of fiber orientation, it was important to orient different layers, or plies, of graphite/epoxy in different directions to achieve strength in more than one direction. Table 3.1.1 lists the proposed ply orientation for some of the major structural components of the aircraft.

Table 3.1.1: Ply Orientation for Selected Structures

	Graphite/Epoxy Ply Orientation
Fuselage	25% at 0°, 50% at +/-45°, 25% at 90°
Wing	25% at 0°, 50% at +/-45°, 25% at 90°
Control Surfaces	50% at 0°, 50% at 90°
Shafts	100% at +/-45°

The wing and body needed strength in all directions, so they have similar ply orientations designed to achieve quasi-isotropic properties. Shafts, on the other hand, undergo primarily torsion, so those plies were oriented to increase shear strength. Finally, the loads on the control surfaces (rudder, elevators and ailerons) will be primarily in tension and compression, hence the ply orientation listed.

3.2 ANALYSIS

Figures 3.2.1 and 3.2.2 show the shear and moment diagrams for the keel beam of the *Condor* in a hover, assuming full fuel and payload weight. In this configuration, positive shear comes from the lift being generated by the main rotor blade, while the negative shear is due to the distributed load of the aircraft weight.

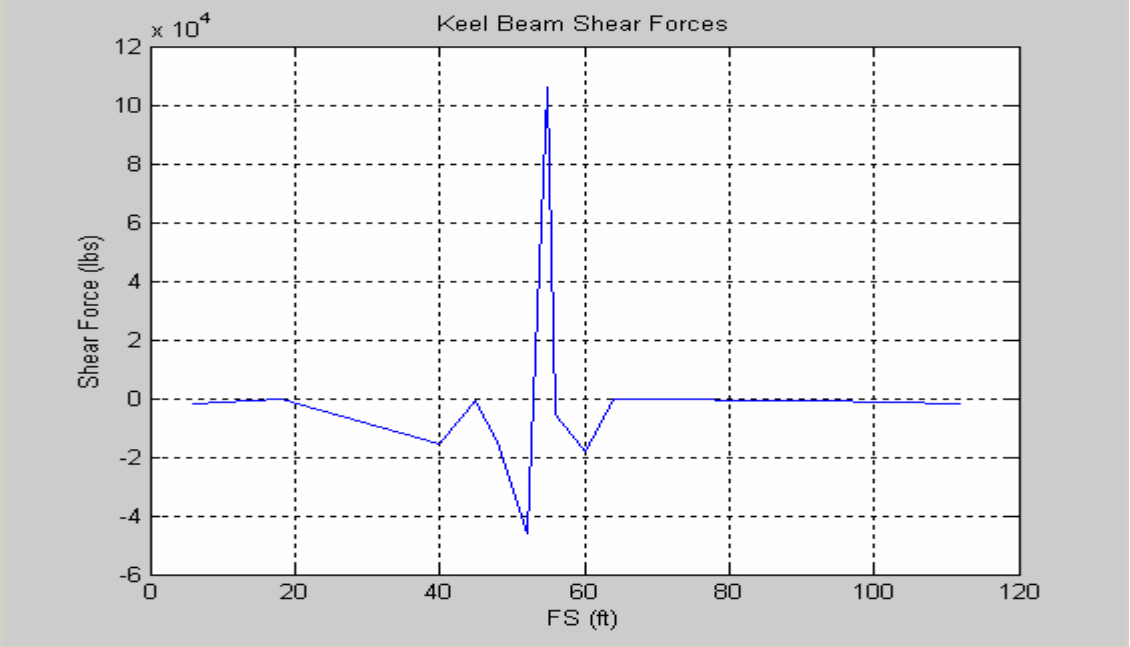

Figure 3.2.1: Shear Diagram

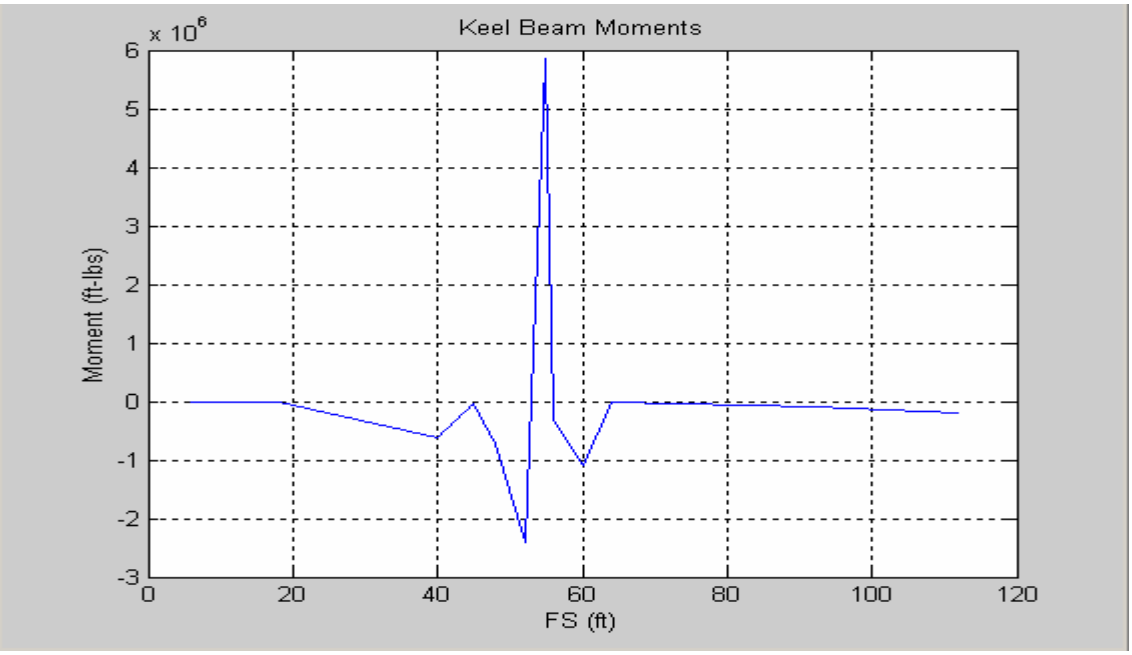

Figure 3.2.2: Moment Diagram

3.3 BODY

As alluded to at the beginning of this chapter, the body was divided into three parts: cockpit, main fuselage, and tail. The primary reason for this was to keep each section under 50 feet in length. This is important because graphite/epoxy is a thermoset resin, so it has to be cured in an autoclave. Hence if large components are not divided into sections, a giant and economically unfeasible autoclave will be needed for the manufacturing process.

The overall shape of the body was driven by several factors: first and foremost, the body needed adequate room in the cargo section to carry the larger vehicles listed in the Initial Requirements Document like the LAV, MTVR and HEMAT. A secondary consideration was to minimize the size of the fuselage. This was primarily done by discarding the circular shape of the original standard C-130J-30 fuselage;

since the *Condor* was not going to be operating above 10,000 feet MSL, there was no need to pressurize the cabin, and therefore no benefit gained from a circular shape. Instead the body evolved into something more resembling a V-22 fuselage.

Each part of the fuselage body will be constructed using a tape lay-up method. First, an aluminum mandrel will be formed in the shape of the fuselage section (including protrusions for bolt holes around the edges of where any two sections will be joined). Then the graphite/epoxy tape will be wrapped around the mandrel, and the entire mandrel will be placed in an autoclave to cure the graphite/epoxy. Finally, the composite section will be removed from the mandrel. Also, since there is inherent weakness surrounding a hole in a composite section, two aluminum "ribs" will reinforce the connections between the three composite sections. Control surfaces like the rudder and elevator will be formed and cured separately, and then attached to the tail section. Construction of the wing will be discussed in the next chapter, but the tape lay-up method will be the same.

3.4 LANDING GEAR

Landing gear data was calculated using Roskam's Airplane Design text (volume II, chapter 9). The basic layout of the landing gear will be a tricycle configuration, with a nose gear and a pair of main gears. Longitudinal tip-over criteria states that the main landing gear must be located behind the most aft c.g. location, usually at an angle of 15°. (See figure 3.4.1.) The most

aft c.g. location of the *Condor* is in its empty condition (no fuel and no payload), in which case the c.g. is at FS 55. This puts the longitudinal position of the main landing gear at FS 56.5.

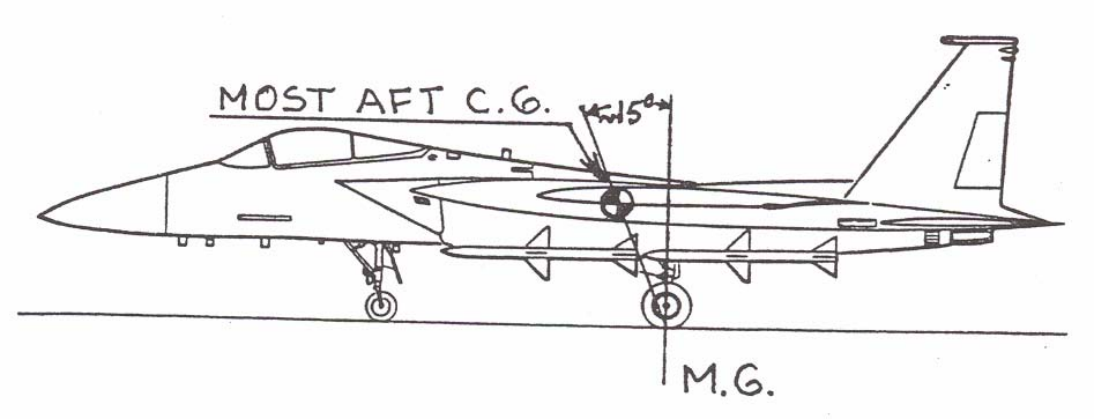

Figure 3.4.1: Longitudinal Tip-Over Criterion

Lateral tip-over criteria states that the main landing gear must be located such that the angle ψ is less than or equal to 55°. (See figure 3.4.2.) By placing the nose gear at FS8, this puts the lateral position of the main gear at 8.5 feet off the centerline, resulting in the main gear being located underneath the aft section of each sponson.

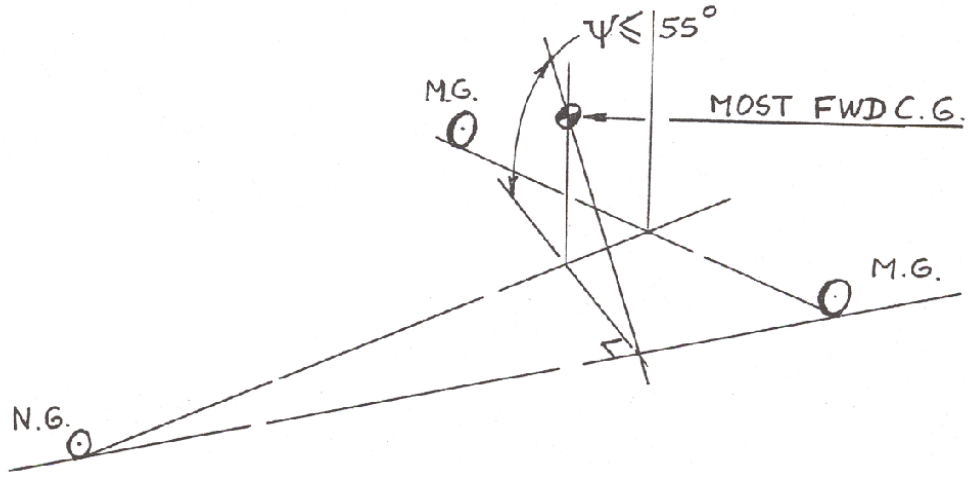

Figure 3.4.2: Lateral Tip-Over Criterion

The remaining data on the landing gear was calculated using equations 9.1 and 9.2, as well as tables 9.1 and 9.2. That data is summarized in the table below:

Table 3.4.1: Landing Gear Data

Landing Gear Data	
Nose Gear	
Number of Tires	2
Tire Pressure	150 lb/in^2
Main Gear	
Number of Struts	2
Number of Tires	2
Tire Pressure	170 lb/in^2

3.5 DAMAGE CONTROL

While this section will be brief, it is important, especially in the case of composites, to discuss some of the basic damage control aspects. For one, composite materials have developed to the point where it is possible to execute a "quick fix" to a structural component by simply welding a piece of metal over a damaged composite section. Also, many of these types of patches are actually being performed now ***with*** composites (Niu, p83). In particular, boron/epoxy is often used as a patch to strengthen a damaged portion of an aircraft. Since epoxy-based composites cure at relatively low temperatures, all that is needed for one of these composite patches is the prepreg material (which must be refrigerated) and a heat lamp.

4. WING

4.1 REQUIREMENTS

The mission for the CH-83 *Condor*, as outlined in the Initial Requirements Document, is to perform a vertical or short take off, travel 100nm over water and 200nm inland, descend vertically to drop off equipment, and return home to the ship. Based on this mission profile, it's obvious that a predominate amount of time will be spent in the airplane mode. For this reason, wing design was critical. In fact, wing design was more important than on previous compound helicopters, because the RVR technology on the *Condor* allows the rotor to be unloaded by 80% in forward flight. Naturally, that 80% is what the wing needs to be designed to lift. With the *Condor* "full-up" at 117,000 lbs, 80% translates to 94,000 lbs.

4.2 COMPOUND WING ATTRIBUTES

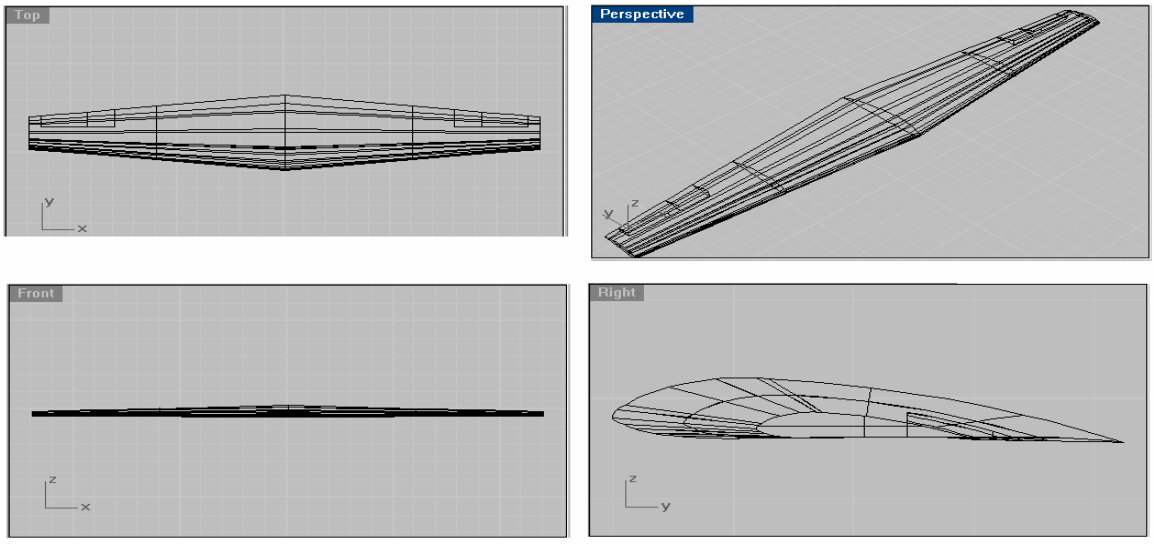

Figure 4.2.1: Compound Wing

The first step in the wing design process was to analyze the cruise conditions. The ***Condor*** is designed to cruise at an altitude of 8000 feet, where it does not have to pay all the structural penalties of pressurizing the fuselage. Based on a similar thought process, its cruising speed will be just over 200 kts, in order to reduce the significant induced drag found at higher speeds.

These two considerations were used to calculate the first wing parameters, using the following simple equation:

$$L = C_L \frac{1}{2} \rho V^2 S$$

In this equation, both the lift coefficient (C_L) and wing area (S) are variables, so initially a of C_L 0.4 was chosen. However, as the design became more detailed the aircraft grew, creating more and more weight to be lifted by the wing, and so increasing the size of the wing. Therefore the C_L was increased to 0.7 in order to keep the wing at a manageable size.

Once the wing area was set at 1250 ft^2, the span and chord were determined by the geometry of the wing. A 0° taper was chosen because the ***Condor*** will never be going near transonic speeds, so sweep is unnecessary. A roughly 50% taper ratio was chosen, in line with historical data on transport or medium-sized aircraft like the C-130 (49%), P-3C (40%), and C-141 (41%). This taper ratio gave a mean aerodynamic chord of 13ft, a root chord of 17ft and a tip chord of 8.5ft. (Data summarized in the table below.)

Table 4.2.1: Compound Wing Parameters

Compound Wing Data	
Parameter	*Value*
Span	96 ft
Mean Chord	13 ft
Area	1250 ft^2
Aspect Ratio	7.38
Taper Ratio	0.48

4.2.1 Wing Location

The wing was mounted high for several reasons. For one, the turboprops used for auxiliary propulsion had to be mounted somewhere, and the wing was the obvious choice. This ruled out the low-wing configuration, which was how the aircraft was initially designed when auxiliary propulsion was going to be provided by Vector Thrust Ducted Fans on the tail end of the aircraft. Discarding the low-wing design also meant that the entire volume of the sponsons (with the exception of some space for landing gear) could be used for fuel storage. From a practical standpoint, a high-wing configuration (vice mid-wing) also allows personnel, troops and cargo handlers to get around the airplane without circumnavigating the 96ft wingspan. (In the final design, the wings sit high on the aircraft at a height of 20ft above the ground.)

There were two other design considerations leading to a high wing design. First, the vertical drag penalty incurred by a compound helicopter with a high-wing design was not noticeably more than a compound with a low-wing design. According to figure 4.2.1 (from Prouty's Helicopter Performance, Stability and Control text), both a high and low-mounted small wing incur a 10% thrust penalty from vertical drag. It can also be seen from this chart that

while wing ***position*** doesn't significantly increase or decrease the vertical drag ratio, wing ***size*** does. Initial designs of the ***Condor*** kept the wing at what would be considered a medium size for this reason. Unfortunately, requirements on the wing increased as the design matured, and the wing had to grow. Second, and finally, the high-wing configuration lends itself to simpler attachment to the aircraft body. This will be discussed in more detail in the final section of this chapter.

4.3 AIRFOIL

The goal of airfoil design was to select an airfoil with good lift at low angles of attack, and low drag at our mission's cruise C_L. The NACA 632-615 airfoil described in table 4.3.1 and pictured in figure 4.3.1 has these characteristics.

Figure 4.3.1: NACA Airfoil

Table 4.3.1: NACA Airfoil Parameters

Airfoil Data	
Parameter	*Value*
Airfoil Type	NACA 63_2-615
Lift Curve Slope	5.73 rad^{-1}
Cruise Lift Coefficient	0.7
Angle of Incidence	2 deg

By choosing an angle of incidence of two degrees, the airfoil achieves the design lift coefficient of 0.7 at zero degrees angle of attack (relative to the aircraft). Also, referring to the drag polar for the airfoil shown in figure 4.3.2, at our cruise C_L of 0.7 the airfoil's drag coefficient is in the "bucket" at about 0.005 or 0.006. (All airfoil data came from Theory of Wing Sections by Abbott.) Due to the very high drag already incurred by our aircraft (mostly due to a large flat plate area), minimizing the drag from the wing was an essential design consideration.

4.4 CONSTRUCTION

As previously discussed, the wing is one of the primary structures of the *Condor* that will be made with composite materials. The goal of building with composites, of course, in addition to reducing empty weight, is to reduce the number of parts. A complex composite part like the outer surface of a wing, for instance, eliminates what used to be several conventional metal pieces and perhaps dozens or hundreds of fasteners.

The composite wing for the *Condor* will be made in three sections – the center section, approximately 48ft in length, and two outer sections, each approximately 24ft in length. Notches will be made in the trailing edge of the two outer sections for the ailerons, which will be the only control surfaces on the wing. (Leading edge flaps and trailing edge flaps being fairly unnecessary on a compound helicopter.) The center section will run through the fuselage, possibly borrowing technology from the V-22 on

how best to accomplish that. It will also have the two turboprops mounted on the outer edges. There are two primary reasons for manufacturing the wing in three sections; first, it keeps each section under 50ft in length. (See the discussion on this in Chapter 4.) The second reason is that the wings need to be able to fold back so that the *Condor* can take up a little less room on the flight deck. This will be discussed in the following section.

4.4.1 Folding and Spot Factor

While a detailed spot factor analysis was not performed on the *Condor*, the IRD did state that the aircraft should have a spot factor between 1.5 and 2 times a CH-53E. The way that criteria was assessed was by using a "deck shadow" method. Essentially, the surface area projected on the deck by a shadow (or rough outline) of the aircraft was used as a numerical representation of the spot factor. This number for a "spinning" CH-53E was assigned a spot factor value of 1.0. The spot factor of the *Condor* was then determined by dividing the *Condor*'s surface are shadow by that of the CH-53E. This "deck shadow" process is summarized in table 4.4.1.

Table 4.4.1: Deck Shadow Calculations

Preliminary Spot Factor Analysis				
		CH-53E	**CH-83**	*(units)*
Main Rotor Radius	R	39.5	55.3	ft
Tail Rotor Diameter	d	20.0	25.0	ft
Est. Elevator Width	w	15.0	48.0	ft
Disc Area	Ad = pi*R^2	4899.5	9607.3	ft^2
Projected Tail Area	At = d*(w+5)	400.2		ft^2
	At = d*w		1200.0	ft^2
Total Projected Area	A = Ad + At	5299.6	10807.3	ft^2
Design Spot Factor	SF	1.0		
Relative Spot Factor	SF		2.0	

As seen from the table, a spinning *Condor* has a spot factor of almost exactly 2 relative to the CH-53E.

Obviously, it will be important to minimize this gigantic area if the *Condor* is going to stay on deck for any length of time. (As will be the case for any ships currently in the Navy's inventory, because the *Condor* is too large for their elevators, so it *can't* be stored below the flight deck.) However, folding was not a criteria laid out in the IRD, so only a preliminary analysis has been done. The folding plan for the *Condor* will affect the wings and the rotors. The rotors will swivel so that all eight blades are lined up over the fuselage. The outer sections of the wings will rotate forward 45° about the midchord, and then fold back and down along main fuselage. (The outer sections of the wing are slightly too long to fold straight down.) With these two modifications, and using the same

deck shadow system as before, the folded *Condor* will have a spot factor equal to just less than 1.1 times a CH-53E.

5. ENGINE AND DRIVE SYSTEM

5.1 REQUIREMENTS

The propulsion system should be able to provide adequate power for the CH-83 *Condor* to perform a vertical takeoff with payload weight of 37,000 lbs at a vertical rate of climb of 200 ft/min in a 4000 ft, 95°F operating environment. It also must have adequate reserve power for the aircraft to perform a safe recovery flight with a single engine inoperative. The propulsion system should also include an auxiliary power unit that could provide electrical and hydraulic power for engine starting, ramp operation and maintenance.

The required power requirement for OGE hover is 22,864 shp in a 4000 ft, 95 F operating environment and 15,485 shp for a standard day. The required continuous power for aircraft cruise at 215 knots is approximately 12,000 shp.

5.2 CONCEPT

Based on the power requirement, a four engine configuration, inclusive of two turboshaft and two turboprop engines, was selected. The four engines will provide a total of 24,300 maximum takeoff shaft horsepower at sea level. The two turboshaft engines provide direct drive to the main gearbox while the power from the two turboprop engines was extracted from the engine alternate drive during hover flight. There is a free-wheel clutch between the connecting shafts from the engine alternate drive to the main gearbox. The two clutches will disconnect

the turboprop engines from the main gearbox to allow the rotor system to decelerates to 50% normal rotational speed during transition to forward flight. The two turboshaft engines will continue to provide power to drive the main rotor at reduced rotational speed. Once the aircraft transits to forward flight, the two turboprop engines will provide the primary propulsion to accelerate and maintain the required forward cruise speed. See Figure 5.2.1 for the proposed configuration.

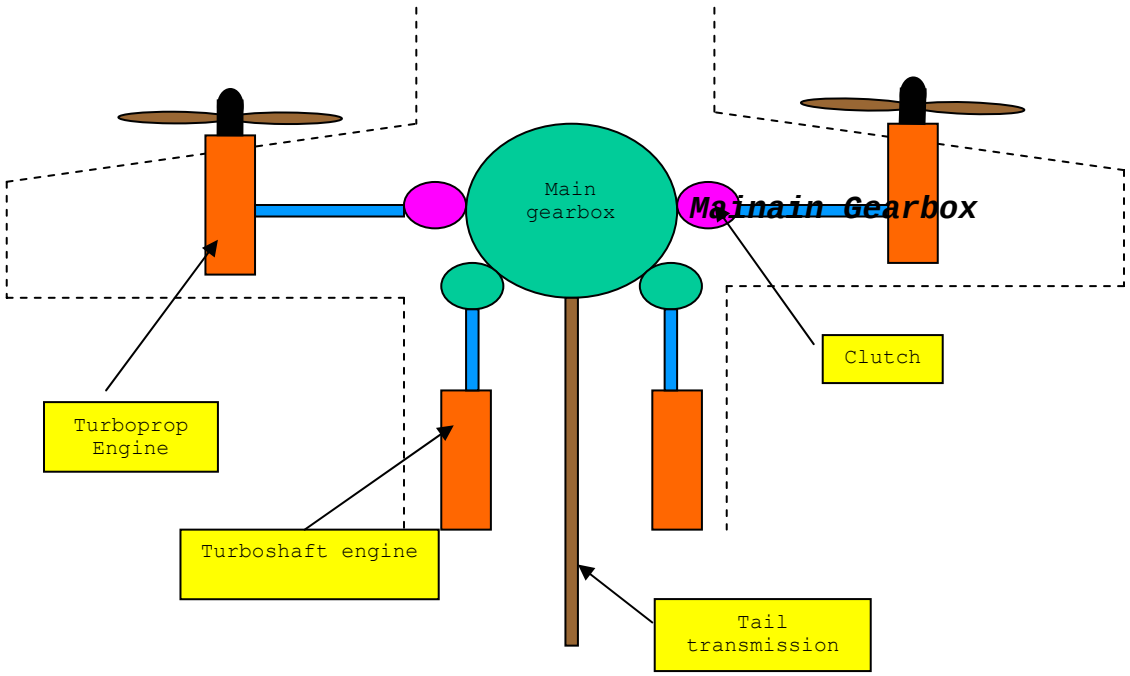

Figure 5.2.1: Proposed Configuration of the CH-83 *Condor* Propulsion System

5.3 ENGINE SELECTION

The principal considerations for engine selection were the ability to meet the required power within the operating

envelope, common core engine for ease of maintenance and minimized cost, lightweight design, and engine control using a state-of-the-art digital control system.

After surveying the engines available in the current market, we have selected the Allison AE1107 turboshaft engine and AE2100 turboprop engine as our final choices. The primary reasons for the selection were as follow:

a. the engine design is modern and has incorporated the latest technology

b. the engine is able to produce the required power

c. the engine core is common for ease of maintenance

d. the engine is equipped with Full Authority Digital Electronic Control (FADEC) for engine control.

The control system is critical for our design, considering the complexity of the requirement to provide both vertical takeoff and forward flight mode with turboprop and turboshaft engines.

5.4 ENGINE DESCRIPTION

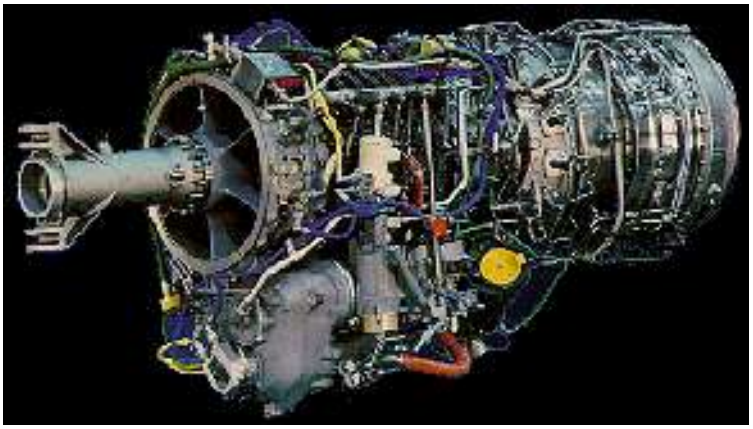

Length x Width x Height	77.08” x 26.40” x 34”
Weight (Dry)	971 lb
Max Power (S/L) up to 43 C	6,150 shp
Maximum Continuous Power (4,000 ft, 25 C)	4,362 shp
Specific Fuel Consumption @ Max continuous power	0.42 lb/hr/shp

Figure 5.4.1: Picture of the Allison AE1107 (US military designation: T406-AD-400)

The Allision AE1107C engine was developed for the tilt rotor V-22 Osprey propulsion system. The advanced technology features include; all-axial high efficiency turbo-machinery components, only four main rotor bearings, positive sump scavenging, modular construction and dual independent Full Authority Digital Engine Control (FADEC). The AE 1107C is capable of developing over seven shaft horsepower per pound of weight - the highest ratio of any engine in its class. Its modern design offers a versatile core common to the AE 2100 turboprop. The core technology benefits from 200 million T56 operating hours across the full range of military operations and over one million hours on the Rolls-Royce AE family of engines.

The two-shaft axial design consists of a 14-stage compressor followed by an effusion-cooled annular combustor, a two-stage gas generator turbine and a two-stage power turbine. It features six rows of variable compressor vanes, dual FADEC, a self-contained oil system that allows for vertical operation, modular construction, and an “on-condition” maintenance capability.

Length x Diameter	108” x 45.3”
Weight (Dry)	1,548 lb
Max Power (S/L) up to 43 C	6,150 shp
Maximum Continuous Power (4,000 ft, 25 C)	4,362 shp
Specific Fuel Consumption @ T/O, SL	0.41 lb/hr/shp

Figure 5.4.2: Picture of the Allison AE2100D3 Turboprop engine

The AE2100D3 turboprop is a two-shaft design with a 14-stage compressor driven by a two-stage HP turbine, the two-stage IP turbine drives the compound planetary reduction gearbox. The engine is the first to use dual FADECs (full authority digital engine control) to control both engine and propeller. The AE2100D3 turboprop engine is rated at 4,591 shaft horsepower. The propeller is made up of an all-composite six-blade R391 propeller system. An automatic thrust control system (ATCS) optimizes the balance of power on the engines, allowing lower values of minimum control speeds during hover flight.

5.5 ENGINE PERFORMANCE

Figure 5.5.1 shows the maximum continuous power while Figure 5.5.2 shows the maximum take-off power for the AS1107C engine. The data source is from NASA-Army Rotorcraft Research Centre.

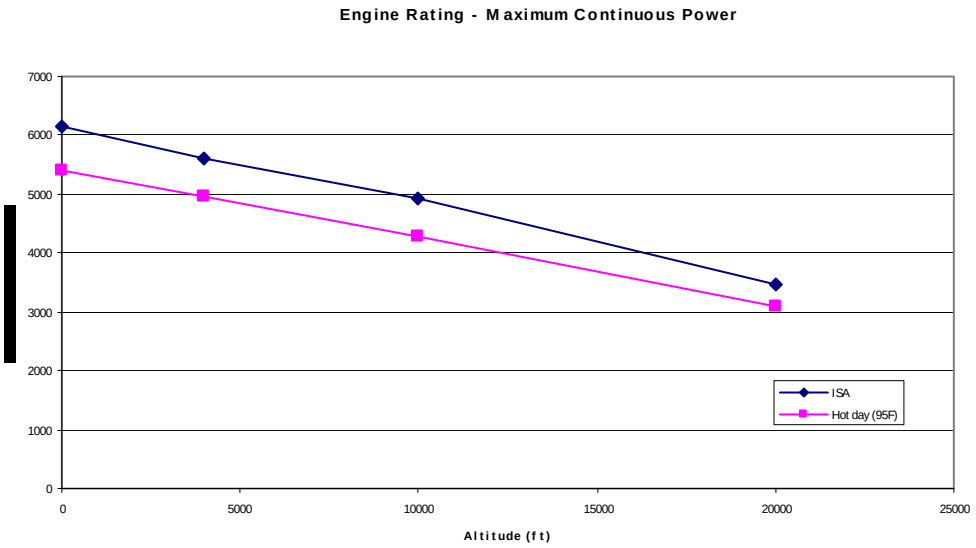

Figure 5.4.1: Engine rating – maximum continuous power

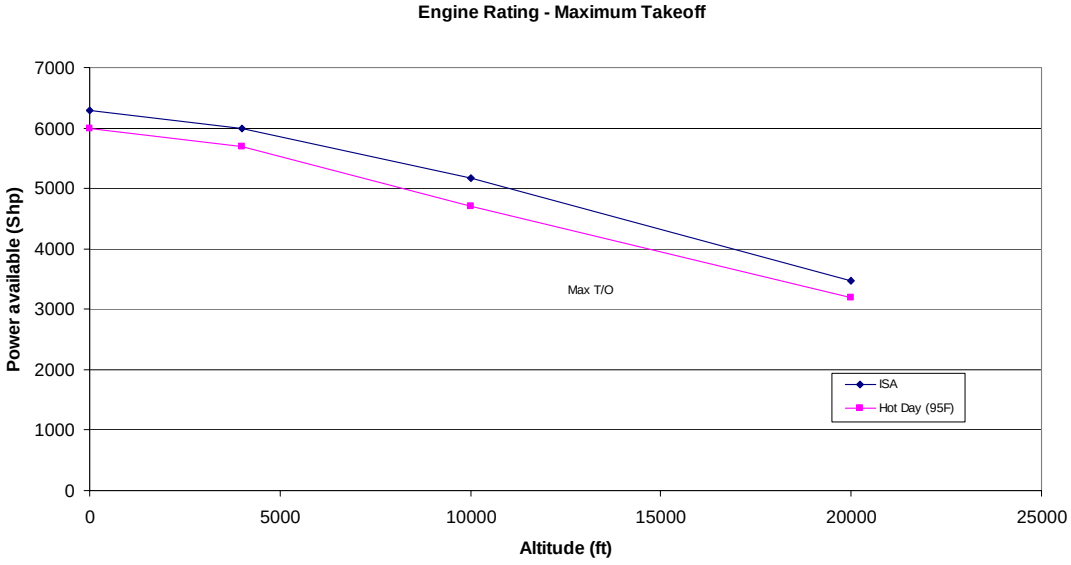

Figure 5.4.2: Engine rating – maximum takeoff power

6. ROTORS

6.1 MAIN ROTOR

The eight-bladed main rotor was designed to lift the aircraft's gross weight at a vertical rate of climb of 200fpm, while performing efficiently in forward speeds exceeding 200kts. Most of the rotor parameters seen in Table 6.1.1 were calculated using an iterative solver that minimized gross weight of the aircraft for the mission. Inherent in this solver was the desire to keep disk loading as low as possible, which not only decreases the power necessary to hover but also decreases problems while operating aboard ships and unprepared landing sites. Another issue in rotor design was the maximum Mach number achieved by the blade tips in forward flight. The rotor blades have a radius of 55.3ft, larger than most modern helicopters, which at forward speeds in excess of 225kts would produce maximum tip Mach numbers greater than 0.90. This is undesirable, as such tip speeds would create shocks over the blade airfoils, creating instability in the rotor system. Since the mission profile demands high forward speeds, it was necessary to slow the rotor down in forward flight. This is achieved by the clutch mechanisms that connect the main gearbox to the drive shafts from the two turboprop engines. As the aircraft increase forward speed, the clutch transfers power to the propellers, which decreases the rpm of the main rotor to a minimum of 50% of that at hover. However, slowing the rotor creates reverse flow over the retreating blades at high forward speeds, as shown in figure 6.1.1, which leads to retreating blade stall. To eliminate this problem, Sikorsky has designed a

double-ended airfoil dubbed the "reverse velocity rotor" (RVR), seen in figure 6.1.2. While only the first harmonic blade angle is normally allowed for helicopter operation, Sikorsky has determined that the second harmonic blade angle is required to operate the RVR airfoil, a feature that compensates for its unique design. Since this airfoil has not been used on a full-scale helicopter, it was necessary to use Sikorsky's performance data on the airfoil for the rotor design. This data from Sikorsky is in the form of the lift per drag curve, seen in figure 6.1.3, which shows a high lift versus drag ratio even at advance ratios greater than one, a feature necessary for the aircraft to achieve its desired performance. Although a design study conducted by Sikorsky shows that a nonlinear planform is optimal for rotor blades, it was decided to use a 1:1 planform blade in this design given that the airfoil has not been used on a full-scale helicopter.

Table 6.1.1: Main Rotor Parameters

PARAMETER	VALUE, HOVER	VALUE, FWD FLIGHT
Number of Blades	8	
Radius (ft)	55.3	
Chord (ft)	4.1	
Hub Radius (ft)	7	
Solidity	0.190	
Direction of Rotation	counterclockwise	
Twist (deg)	-8	
Taper (root/tip)	1:1	
Blade Loading (psf)	74.6	
Flatwise I_{xx} (in^4)	42	
Edgewise I_{yy} (in^4)	460	
A_s (in^2)	16.5	
Rotational Velocity (rpm)	105.3	52.7
Maximum Tip Mach #	0.55	0.61
% Lift Generated by Rotor	100	20

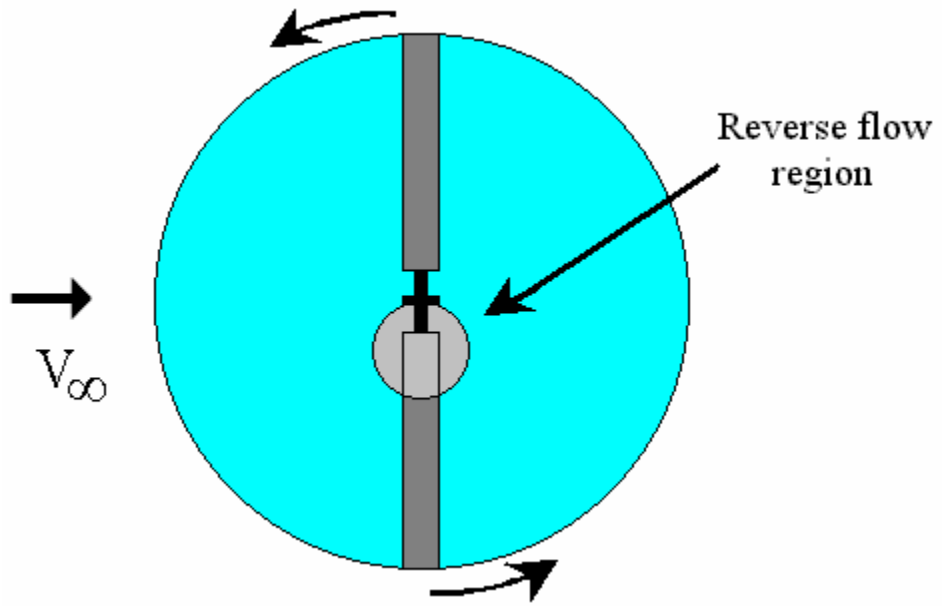

Figure 6.1.1: Reverse Flow on a Rotor Disc

Figure 6.1.2: Reverse Velocity Rotor Airfoil

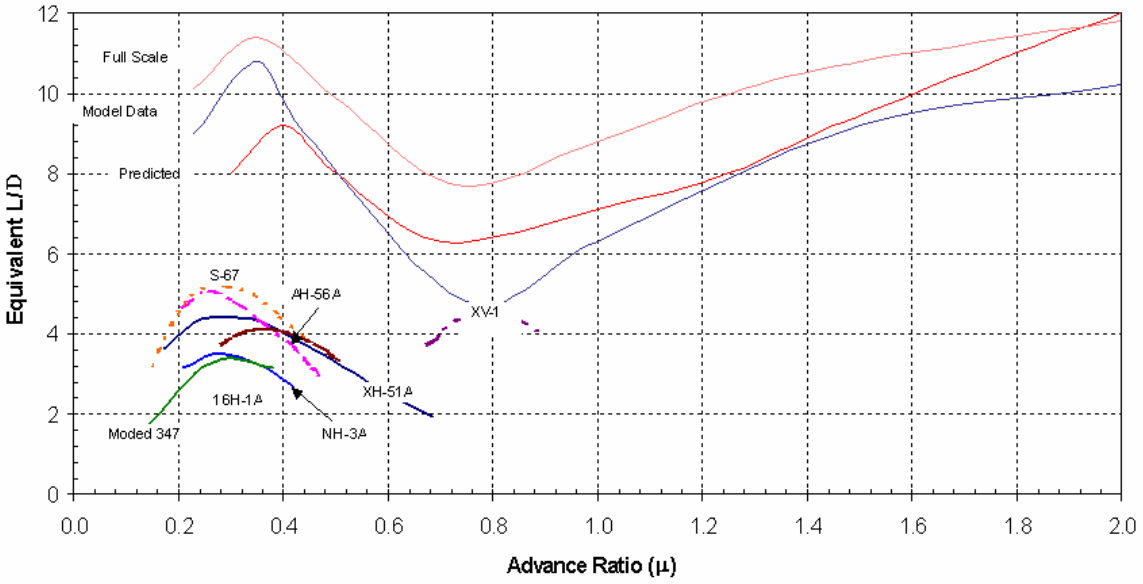

Figure 6.1.3: L/D vs. Advance Ration for RVR Airfoil

6.2 MAIN ROTOR DRIVESHAFT

The driveshaft parameters are listed in table 6.2.1. Two short shafts of length 4ft deliver power from the two turboshaft engines to the main gearbox, and two more shafts of length 22.3ft deliver power from the turboprop engines. The driveshafts are clamped-clamped beams composed from the titanium alloy Ti-6A1-4V, chosen for its high strength-to-weight ratio. The number of segments, outer radius of the shafts, and thickness of the shafts were calculated to minimize the weight of the shaft and the maximum shear stress of the shaft. Also a factor in the shaft design was to ensure the rotational velocity of the shafts was not the same as the natural frequency of the shafts. The power transmitted by the shaft is the product of torque and rotational velocity, thus the faster the shaft rotates the less torque is required to be transmitted for a given power. With the given overall shaft length and the required overall rotor power in hover of 17340hp, the turboshaft driveshafts were designed with an outer radius of 1.00in and a thickness of 0.2in. The turboprop driveshafts were divided into four interchangeable sections, with an outer radius of 1.00in and a thickness of 0.1in. Flexible couplings join the driveshaft sections. The total weight of the driveshafts from the turboshaft engines is 8.5lb each, and the turboprop driveshafts weigh 25.5lb each.

Table 6.2.1: Driveshaft Parameters

	Long Shafts	TS Short Shafts	TP Short Shafts
Length (in)	272	48	89
Number of	3	2	6
Total Volume (in^3)	456	29	53
Angular velocity ω (rpm)	**600**	**6000**	**5280**
Material	**Titanium Alloy (Ti-6A1-4V)**		
Torque (lb in)	266281	45536	51745
Power (shp)	**2535**	**4335**	**4335**
Outer radius $c_{o\ (in)}$	1.433	1.000	1.000
Inner radius $c_{i\ (in)}$	1.233	0.900	0.900
thickness (in)	0.200	0.100	0.100
Max. Shear Stress (psi)	127456	84294	95789
Approx. Mat'l Yield Shear Stress (psi)	87		
Weight	219	9	51

6.3 MAIN ROTOR GEARBOX

The engines drive the main rotor transmission, which drives the main and tail rotors and accessories. The main gearbox is composed of two stages. In hover, the first stage, the input module, receives input shafts turning at 1500rpm from each turboshaft engine and 1140rpm from each turboprop engine. This stage outputs at 600rpm. The main module to the main rotor receives the 600rpm from the input module and outputs 113.5rpm to the main rotor. As aircraft forward speed increases and the clutch assemblies unload the rotor, the rotational velocity to the main rotor decreases to a minimum of 52.7rpm.

6.4 TAIL ROTOR

The tail rotor was designed to counter the 864,873 ft-lb of torque produced by the main rotor. The tail rotor has 6 blades with a diameter of 25ft and a chord of 1.31ft, which at its position 68ft aft of the main rotor necessitates it produce a side force of 12,719lb. This is achieved by a rotational speed of 602 rpm, which requires 2535hp. At this rotational speed, the tail rotor sees a maximum tip Mach number of 0.7. When the rotor is unloaded, the tail rotor is also unloaded as well and has a minimum rotational velocity of 341 rpm.

6.5 TAIL ROTOR DRIVESHAFT

The tail rotor driveshaft transfers power from the input module of the main gearbox a distance of 68ft to the tail gearbox. The tail rotor shaft was designed with the same material as the main rotor shafts. The number of segments, outer radius of the shafts, and thickness of the shafts were calculated to minimize the weight of the shaft and the maximum shear stress of the shaft. Also a factor in the shaft design was to ensure the rotational velocity of the shafts was not the same as the natural frequency of the shafts. The power transmitted by the shaft is the product of torque and rotational velocity, thus the faster the shaft rotates the less torque is required to be transmitted for a given power. With the given overall shaft length, the necessary rotational velocity of 600rpm, and the required power of 2776 shp, the shaft was divided in to three 22.7ft interchangeable sections with an outer radius of 1.43in and a thickness of 0.2in. Flexible couplings join the driveshaft sections. Each segment of the driveshaft weighs

73lb, which gives a total shaft weight of 219lb.

6.6 TAIL ROTOR GEARBOX

The tail gearbox receives input from the tail driveshaft at 600rpm. The tail rotor drive is turned 90° to drive the fan using a single stage worm gear with a 1:1 ratio.

7. AUXILIARY PROPULSION

7.1 PROPELLER SIZING

The actual details of the propeller design, such as the blade shape and twist, are not required to layout the propeller-engine aircraft design. However, the diameter of the propeller, the dimensions of the engine and the locations of intake and exhaust need to be determined in the initial design.

Generally speaking, the larger the propeller diameter, the more efficient the propeller will be. The limitation on length is to keep the propeller tip speed below sonic speed. At sea level, the helical tip speed of a metal propeller should not exceed 950 fps.

To determine the rotor diameter, the following formula (Roskam, Aircraft Design II, Page 128) was used:

Dp = Sqrt(4 * Max Engine Power / Pi * No. of propeller blades * Power loading per blade)

As for our configuration,

Max engine power = 4500 Shp

No. of propeller blades = 6

Power loading per blade = 5.828 Shp/ft^2 (From C-130J turboprop engine reference)

Therefore, the diameter of the propeller is **12.8 ft**.

The tip speed was checked by the following formula:

$(V_{tip})_{helical} = Sqrt\ (V^2_{tip} + V^2)$

where (V_{tip}) = Pi * n * d = 3.14 * 6 * 12.8 ft = 241.3 ft/s

Therefore,

V = Cruise speed = 205 knots = 346 ft/sec

$(V_{tip})_{helical} = Sqrt\ (241.3^2 + 346^2) =$ **421.83 ft/sec**

The tip speed was shown to be less than sonic speed of 950 fps. Propeller design is satisfactory.

7.2 PROPELLER LOCATION

Wing mounting of the engine was recommended for multi-engine designs. Wing mounting of engine reduces wing structural weight through span loading effect, and reduces fuselage drag by removing the fuselage from the propeller wake.

However, wing mounting of engines introduces engine-out controllability issue that force an increase in the size of the tail rotor yaw control and vertical fin. In addition, due to the location of the turboprop engines, the turboprop engine will be susceptible to sand ingestion during hover. Therefore, we have installed additional sand particle separators as part of the engine intake to eliminate the problem.

8. PERFORMANCE

A helicopter performance analysis is made typically to answer the questions of; how high? How fast? How far? and how long? This chapter deals primarily with those questions. The performance of the designed helicopter generally can be classified under hover, vertical climb, forward flight, maneuvering flight and auto-rotation performance. The performance of the *Condor* was primarily computed using JANRAD. This development tool uses blade element theory to determine rotor forces and moments, and a method for harmonically balancing the forces and moments to adjust cyclic pitch. JANRAD had been validated against flight data of other helicopter before and proven to be reliable.

8.1 HOVER

The hover induced velocity distribution was determined by implementing the section of the JANRAD code that predict hover performance. Hover inflow is calculated by equating blade element thrust with momentum thrust in the code. Blade element theory is then used to compute the rotor power required and rotor torque. In all the hover calculations, downwash on the vertical projected area was accounted for. Figure 8.1.1 shows the HOGE power required/available for Army hot day of pressure altitude of 4000 ft and ISA 95°F versus G.W. Sizing of engines was based on the most demanding flight regime, cruise flight in excess of 200 knots.

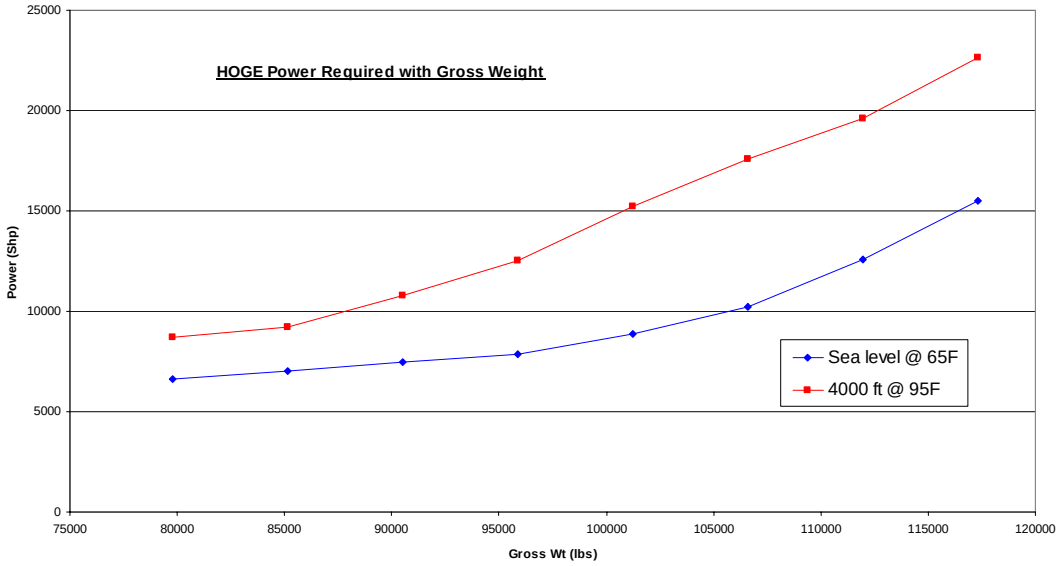

Figure 8.1.1: HOGE power required for hot day of pressure altitude of 4000 ft and sea level versus G.W

8.2 VERTICAL CLIMB

The change in energy required with the excess power available was used to calculate the vertical climb performance. All necessary vertical drag, downwash and tip losses were all taken into account. Vertical rate of climb was plotted against airspeed in Figures 8.2.1 through 8.2.3.

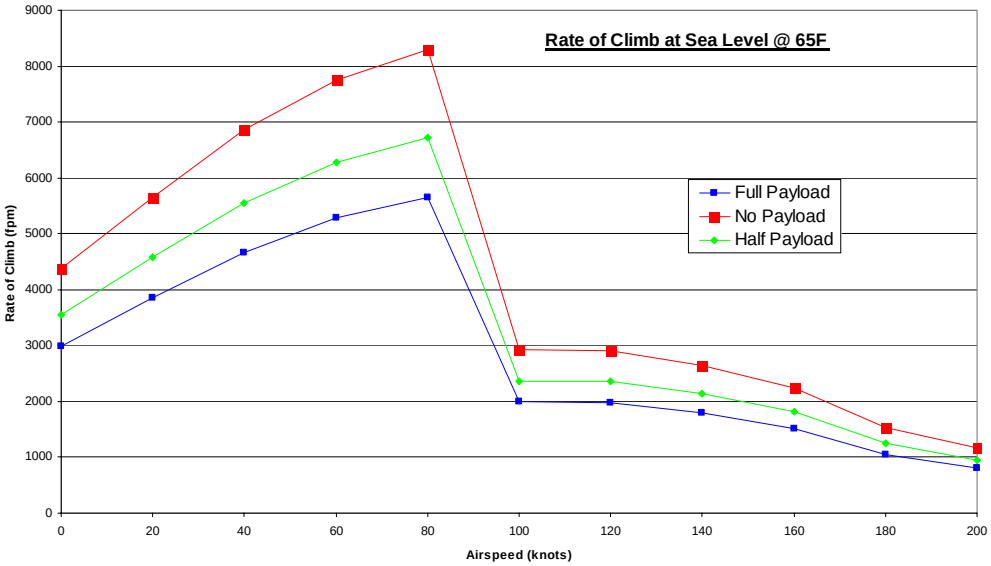

Figure 8.2.1: Vertical rate of climb variation with airspeed at sea level

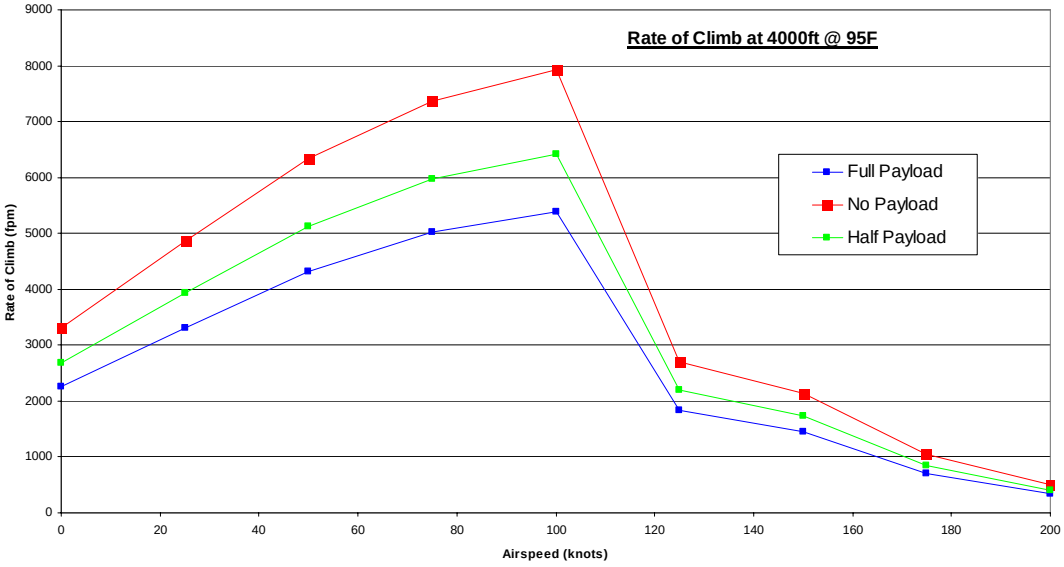

Figure 8.2.2: Vertical rate of climb variation with airspeed at altitude 4000ft

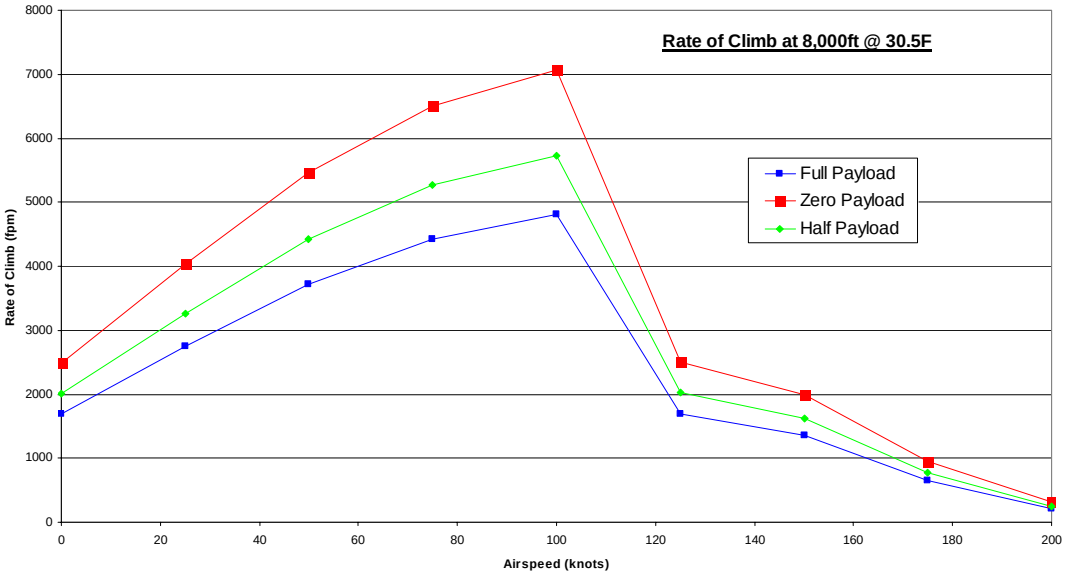

Figure 8.2.3: Vertical rate of climb variation with airspeed at altitude 8000ft

8.3 FORWARD FLIGHT

Forward level flight was calculated by JANRAD using blade element theory. Figures 8.3.1 through 8.3.3 shows power required variation with airspeed at different altitude.

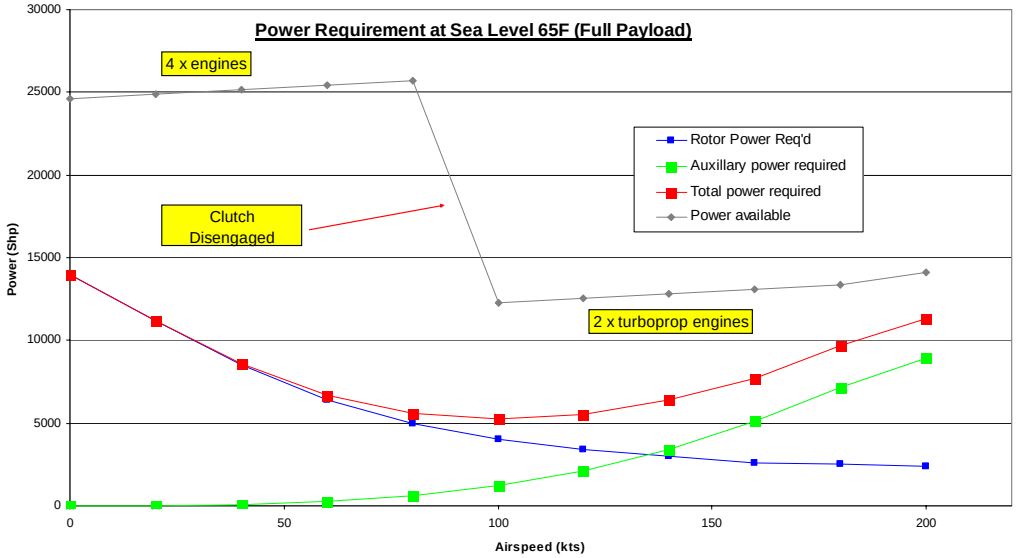

Figure 8.3.1: Power required variation with airspeed at sea level

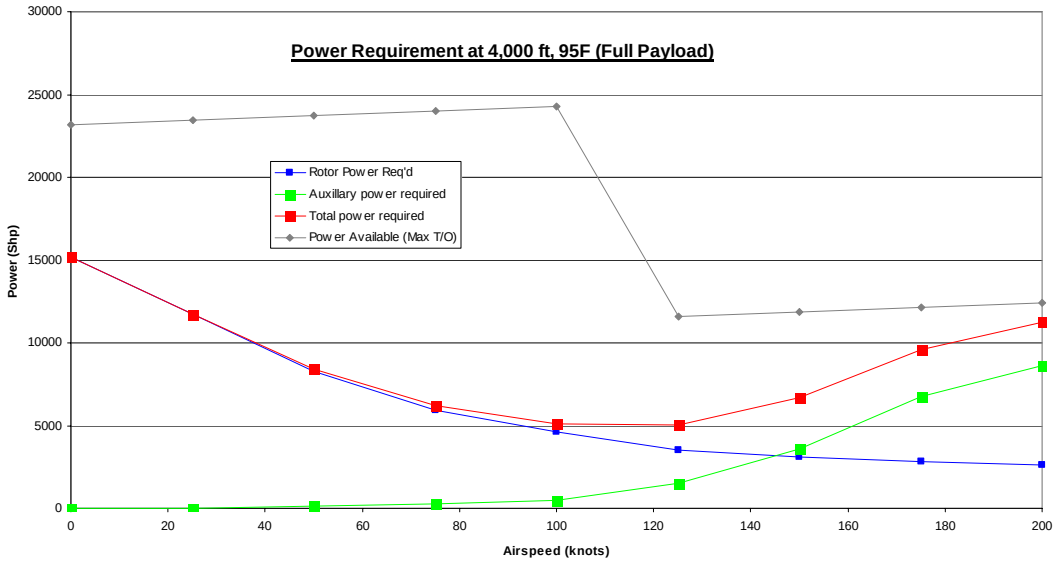

Figure 8.3.2: Power required variation with airspeed at altitude 4000 ft

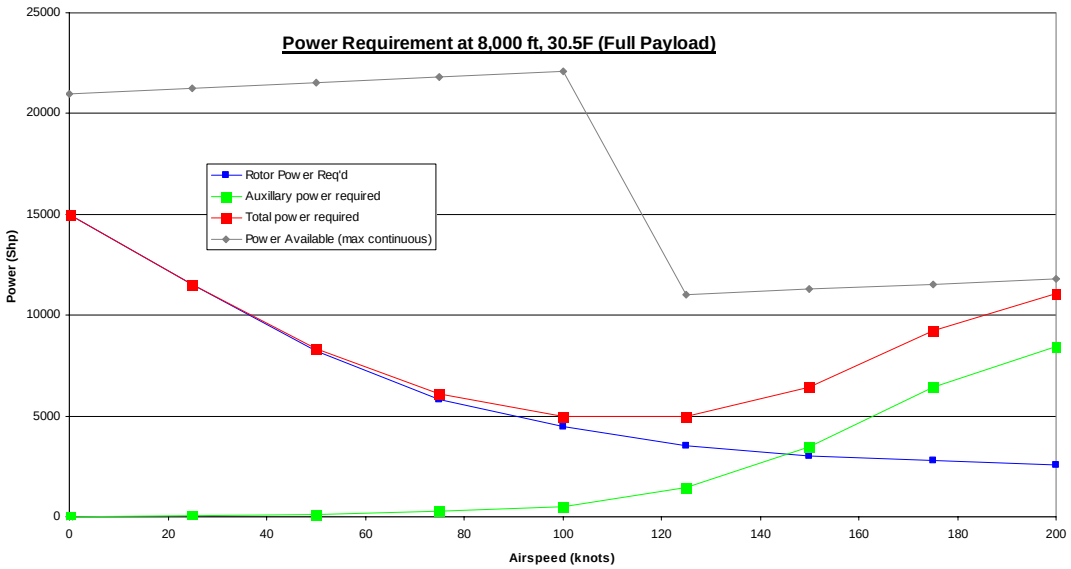

Figure 8.3.3: Power required variation with airspeed at altitude 8000 ft

8.4 MANEUVERING FLIGHT

The G.W. and the main rotor blade weights were varied to simulate maneuver severity. The level flight trim iteration was then performed. Using a standard 30° bank angle turn, this resulted into a 1.2 g requirement; which well within the maximum sustained load factor at anticipated cruising altitudes. Figure 8.4.1 shows the V-N diagram of the *Condor*, this was generated from interactive software from the internet based G.W and pressure altitude.

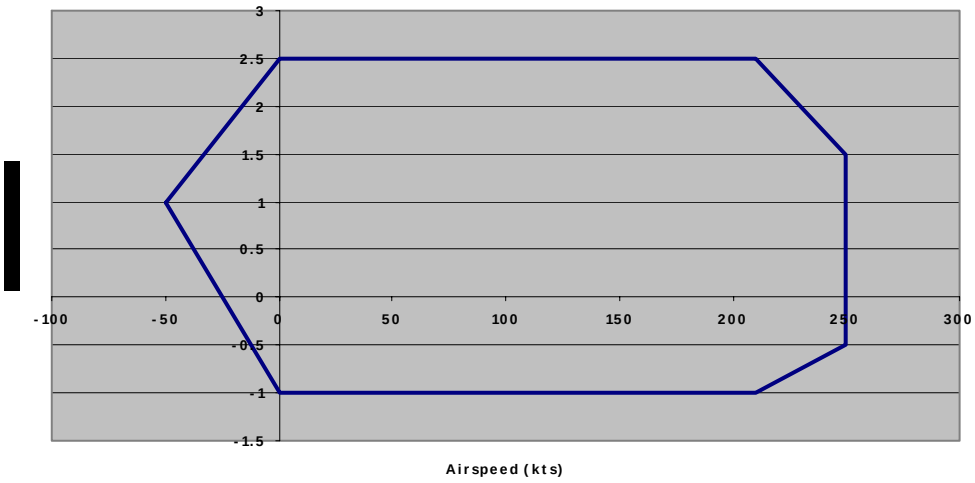

Figure 8.4.1: V-N diagram of the ***Condor***

9. DYNAMICS

9.1 STATIC ROLLOVER

The maximum surface angle upon which a helicopter can rest statically is an important measure of the helicopter's ability to survive on a rolling ship. Static rollover takes into account static forces only. The static angle for the *Condor* was found to be 33.18 degrees.

9.2 STABILITY AND CONTROL

Hover handling qualities, for this aircraft, were evaluated to assess the inherent stability of the airframe. Stability derivatives were calculated and analysis performed using version 6.0 of the Joint Army/Navy Rotorcraft Analysis and Design program (JANRAD). JANRAD uses a linearized state space, six degree-of-freedom representation based on the NASA results presented in NASA TM 84281. The dynamics model of the helicopter is represented in state space format as a matrix differential equation (9.2.1):

$$\dot{X} = [A]X + [B]u \qquad (9.2.1)$$

Where the state vector X = [u w q θ p φ r]^T and the control vector u = [δ_{long} δ_{coll} δ_{lat} δ_{ped}]^T.

Calculation of the hover stability derivatives for the aircraft is based on Prouty's textbook ***Helicopter Performance, Stability, and Control***. Prouty uses a graphical method to determine relationships that define stability derivatives. JANRAD determines the derivatives through an iterative process by perturbing the parameters μ,

θ_0, and λ' independently and computes the values for the variables C_T, C_H, C_Q, a_{1s}, and b_{1s}. The results presented by JANRAD include the eight by eight plant matrix and an eight by four control input matrix. These results allow comparison with the Army's Aeronautical Design Standard, ADS-33D.

Open loop stability was evaluated in hover on a high, hot day. Tables 9.2.1 through 9.2.3 present open loop eigenvalues, damping and natural frequencies for the hover case. As expected, open loop characteristics are unstable as indicated by positive eigenvalues. The eigenvalues are presented in figures 9.2.1 through 9.2.3. In a hover, the *Condor* meets Level 2 handling qualities. The Stability Matrices are given in figure 9.2.4.

Table 9.2.1: Coupled Open Loop Characteristics

Coupled Characteristics		
Eigenvalue	Damping Ratio	Natural Frequency (rad/s)
-13.28	1	13.280
-2.12	1	2.120
-0.65	1	0.650
-0.19	1	0.190
0.36 + .39i	-0.678	0.531
0.36 - .39i	-0.678	0.531
0.36 + 1.19i	-0.290	1.243
0.36 - 1.19i	-0.290	1.243

Table 9.2.2: Uncoupled Longitudinal Characteristics

Uncoupled Longitudinal Characteristics		
Eigenvalue	Damping Ratio	Natural Frequency (rad/s)
-0.44	1	0.440
-0.12	1	0.120
0.18 + .36i	-0.447	0.402
0.18 - .36i	-0.447	0.402

Table 9.2.3: Uncoupled Lateral Characteristics

Uncoupled Lateral Characteristics		
Eigenvalue	Damping Ratio	Natural Frequency (rad/s)
-13.22	1	13.220
-2.12	1	2.120
0.24 + 1.07i	-0.219	1.097
0.24 - 1.07i	-0.219	1.097

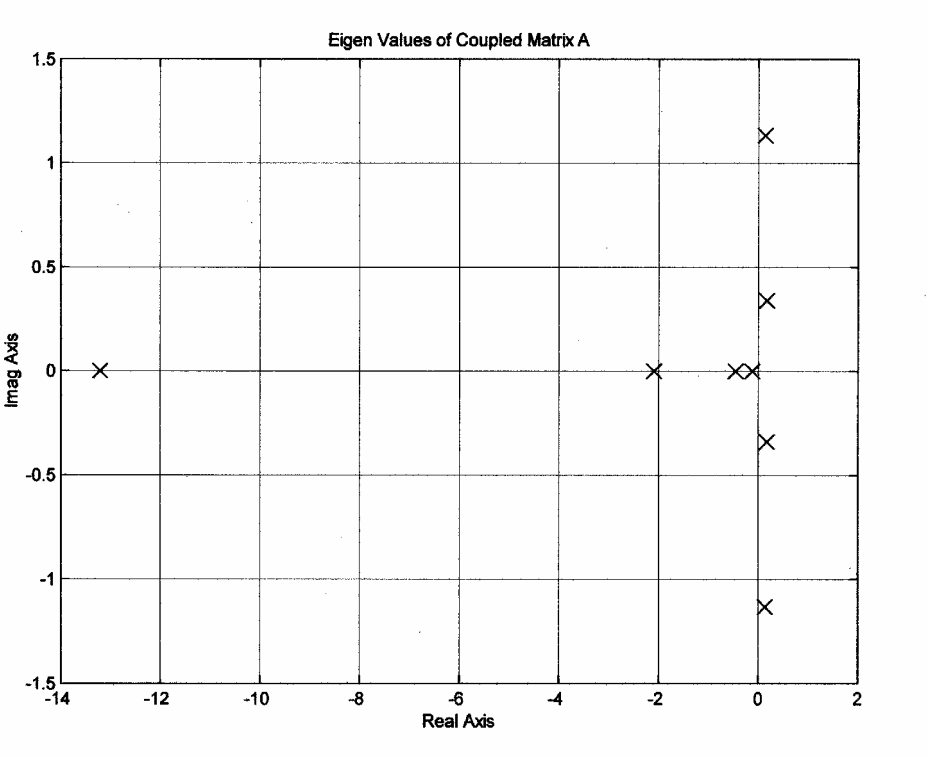

Figure 9.2.1: Coupled Eigenvalues

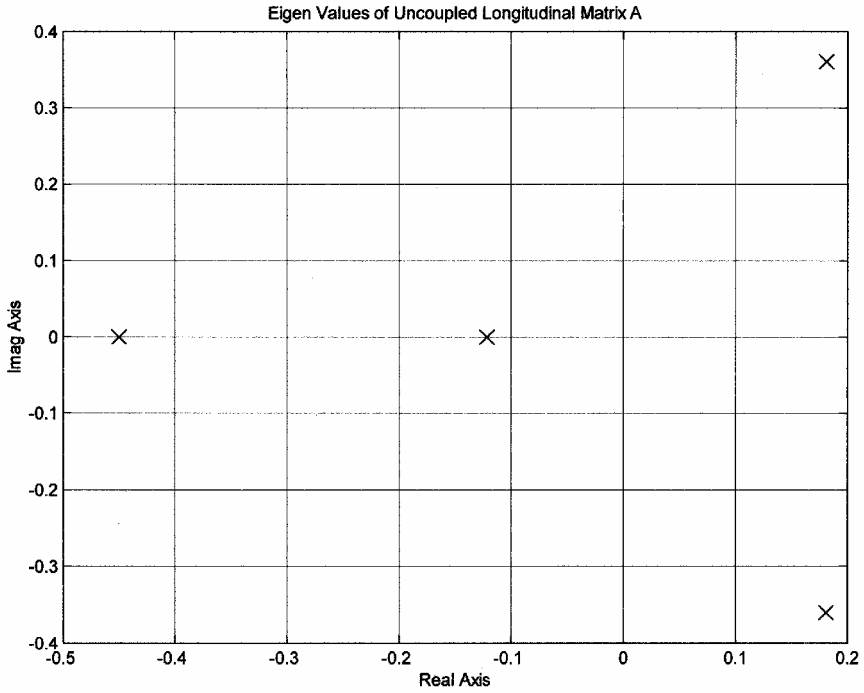

Figure 9.2.2: Uncoupled Longitudinal Eigenvalues

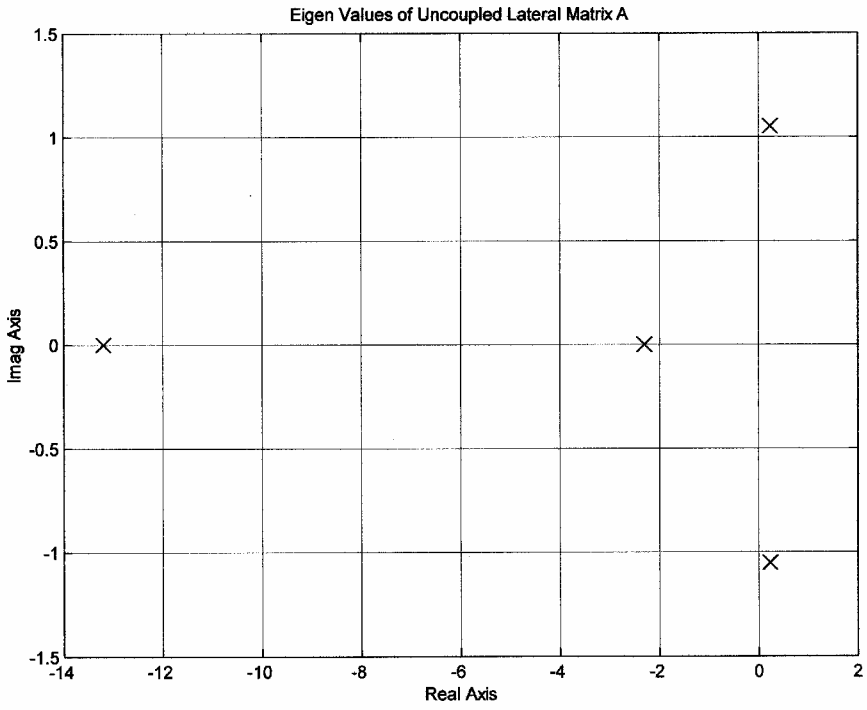

Figure 9.2.3: Uncoupled Lateral Eigenvalues

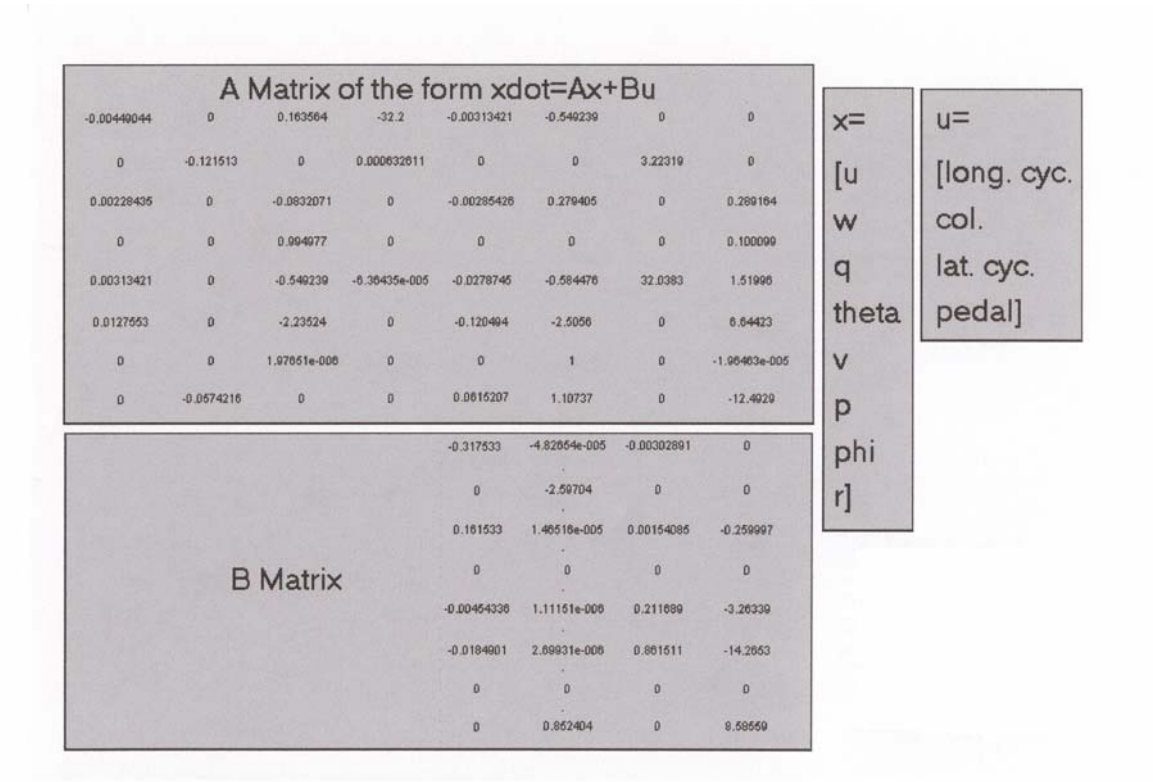

Figure 9.2.4: Stability Matrices in Hover

In forward flight the ***Condor*** was assumed to act as an airplane instead of a helicopter. A preliminary study of the aircraft's static stability derivatives was conducted. For longitudinal static stability the cg must remain in front of the neutral point. The neutral point, static margin and the worst cg (no load, no fuel) are given in Table 9.2.4.

Table 9.2.4: Static Margin

Neutral Point	0.68%mac
Worst Case cg	0.52%mac
Static Margin	0.15%mac

Weathercock Stability ($C_{n\beta}$) is the yawing moment produced given a sideslip angle (β). $C_{n\beta}$ must be positive to produce a yawing moment that restores the aircraft to

symmetric flight. Dihedral effect (C_{l_β}) is the tendency to roll when disturbed from stabilized flight (gust). C_{l_β} must be negative to produce a rolling moment back to wings-level. Table 9.2.5 gives the static stability derivatives for the *Condor*.

Table 9.2.5: Static Stability Derivatives

Weathercock Stability	0.0065/deg
Dihedral Effect	-0.0025/deg

9.3 SUMMARY

As expected, the *Condor* in helicopter mode is unstable and will require a stability augmentation system. The airplane mode of this aircraft was found to be statically stable, yet still controllable. A closed loop system was not studied for this conceptual design; this is a requirement for further study into this aircraft.

10. WEIGHT AND BALANCE

The key factor in the design of the helicopter is the weight sizing. Detailed weight sizing is based on extensive previous experience and good judgment about existing and future engineering trend. Weight equation of specific helicopter components are derived from other same 'class' vehicles and subjected to a mathematical process known as the multiple linear regression which determines sensitivities with respect to every parameter that logically affects the weight of the component.

10.1 WEIGHT ESTIMATION

The set of equations in Appendix A were found to be suitable for the weight estimate of the designed helicopter after verifying the set of equations with data from the MI-26 helicopter.

Table 10.1.1: A summary of the group weight computed

	Group weight (lbs)
Rotor	10157
Tail rotor	1835
Body	15186
Alighting gear	2265
Nacelle	4861
Propulsion	7764
Drive System	11409
Flight Controls	232
Auxiliary power plant	300
Instruments	1715
Hydraulic	306
Electrical	723
Avionics	400
Furnishing and equipment	5368
Door Mechanism	1000
Air Cond & anti ice	938

Manufacturing variation	469
Total empty weight	**64928**

10.2 CENTER OF GRAVITY

The longitudinal position of the center of gravity of the empty designed helicopter is calculated from the sum of the static moments about some arbitrary point contributed by each group (in Table 10.1.1) that makes up the empty weight divided by that weight. The arbitrary point that was selected was the nose of the helicopter. Table 10.2.1 shows the calculation of the position of the center of gravity. Note that as the design proceeds towards a more advanced stage, this calculation would become more and more precise by expanding it to account for the weight and location of each and every component of each group.

Table 10.2.1: Summary of the CG position calculation

	Group weight (lbs)	Fuselage station (ft)	Moment (ft-lbs)
Rotor	10157	48.0	487531.38
Tail rotor	1835	112.0	205545.16
Body	15186	60.0	911150.64
Alighting gear	2265	60.0	135874.98
Nacelle	4861	48.0	233341.39
Propulsion	7764	52.0	403752.69
Drive System	11409	55.0	627471.75
Flight Controls	232	52.0	12065.29
Auxiliary power plant	300	64.0	19200.00
Instruments	1715	6.0	10287.13
Hydraulic	306	52.0	15931.71
Electrical	723	45.0	32519.98
Avionics	400	18.0	7200.00
Furnishing and equipment	5368	56.0	300620.40
Door Mechanism	1000	92.0	92000.00
Air Cond & anti ice	938	60.0	56302.74
Manufacturing variation	469	52.0	24397.85
Total empty weight	64928	Total moment	3575193.09
Longitudinal CG	**55.064ft**		
% of MAC	**61.99%**		

10.3 CENTER OF GRAVITY TRAVEL

When the aircraft is carrying a payload, the overall CG will be different than when it is unloaded. Figure 10.3.1 plots the overall gross weight of the aircraft as a function of the center of gravity for the different load cases studied in Chapter 2. There are two important trends to notice in this graph. First, for each of the seven load cases at both full and half fuel, the CG of the aircraft remains between 20 and 40 percent of the mean aerodynamic chord. From an airplane stability point of view this translates to an extremely stable, and controllable aircraft, no matter what load is being carried. Second, each load case is located roughly a few feet behind fuselage station 48 feet, which is the center of the main rotor. From a helicopter stability point of view this translates to a dynamically stable helicopter. Thus, despite the CG travel, desirable stability qualities are found at both low and high speeds, in helicopter and airplane mode. Additionally, for all possible load and no load configurations, the overall CG of the aircraft remained ahead of the neutral point. This further adds to the beneficial stability qualities of the aircraft.

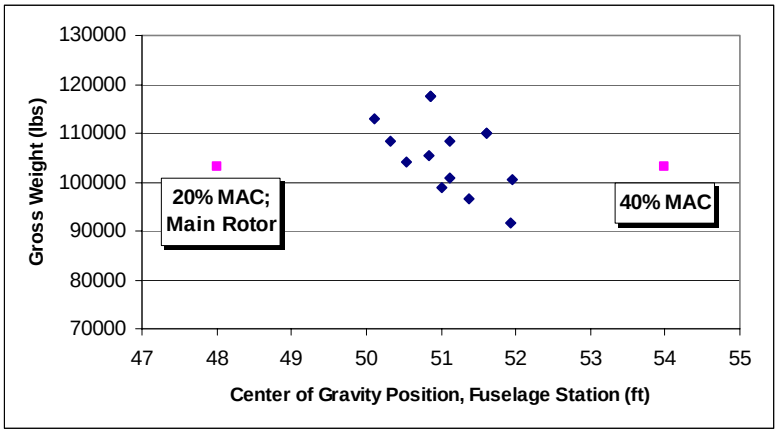

Figure 10.3.1: CG travel locations

11. SURVIVABILITY

Many survivability features are incorporated in the *Condor*. A detailed analysis of susceptibility and vulnerability is beyond the scope this preliminary design report but this section will briefly discuss susceptibility and vulnerability reduction feature and their effects on aircraft survivability.

11.1 SUSCEPTIBILITY REDUCTION FEATURES

All aircraft survivability equipment discussed in Section 2.1.7 is incorporated into *Condor's* design. These active systems are integrated with the following passive measures to reduce aircraft signature.

11.1.1 Radar

Reduction of radar cross section (RCS) is an important susceptibility reduction measure. The following features are used to reduce the RCS.

a. Use of Radar Absorbent Material (RAM) on the leading edges of the compound wing, tail sections, engine inlets, and the sponsons.

b. Indirect path through the inlets to the engine compressor section.

c. Retractable landing gear system.

11.1.2 Infrared Signature

Passive reduction in the IR signature is accomplished through the use of an IR suppressor engine exhaust system

that mixes ambient temperature air with the hot exhaust gases to reduce the temperature of the exhaust as it exits the engine fairings. Additionally low IR paint is used on the fuselage and wings to reduce glint and hot spots.

11.1.3 Visual/Auditory

Due to *Condor's* large size visual reduction is no easy task. A two tone paint scheme similar to that used on Air Force transports is used to increase visual acquisition and tracking range. To reduce sun glint, the cockpit window and cargo compartment windows are covered with a low reflective coating. Although rotor noise will be significant while at low airspeeds and hovering only a fraction of that noise will be present at cruise speeds. Turbo-machinery noise will be masked by mounting the engines and drive systems inside fairings.

11.2 VULNERABILITY REDUCTION

The following vulnerability reduction features are incorporated in the design:

a. Ballistic hardening and shielding.

b. System and component redundancy with separation.

c. Protection of critical components through separation.

d. Reduction of critical components.

The following section briefly discusses the integration of these vulnerability reduction features into major aircraft subsystems.

11.2.1 Cockpit

The lower half of the cockpit is shielded by a ballistically tolerant KEVLAR blanket. A KEVLAR plate will provide protection to the avionics bay. Flight controls are fully redundant in both sides of the cockpit and any one of the flat panel displays can be configured to display critical flight or tactical data.

11.2.2 Flight Controls and Main Rotor System

The fly-by-wire control system includes two separated and protected Flight Computers with multiple electrical control paths and dual power supplies. The entire control system is made up of 23mm round fragment ballistically tolerant control actuators. Both the main rotor and the tail rotor are 23 mm round fragment tolerant.

11.2.3 Auxiliary Propulsion System

The auxiliary propulsion system engines are contained within nacelles augmented with KEVLAR blankets shielding critical components. A blast shield between the engines and the wing structure contains damage. The propellers are design to be 23mm round fragment tolerant.

11.2.4 Fuselage Mounted Engines/Drive Train

The two fuselage mounted engines provide redundancy with separation. A ballistically tolerant blast shield is mounted between the engines and critical drive train components. Additionally, each engine has an independent armor plate mounted to the compressor and turbine section to shield against blast fragments and to contain internal explosions. The engines possess the capability to run dry for up to five minutes. The main transmission and tail rotor gearboxes are ballistically tolerant up to 12.7mm. The main transmission can run dry for up to 30 minutes. The tail rotor gearboxes can run dry for up to 20 minutes. All drive shafts are shielded by either aircraft structure or ballistic blankets. The drive shafts to the main rotor and tail rotor are 23 mm ballistic tolerant. The drive shafts from the auxiliary propulsion system are 12.7mm ballistic tolerant.

11.2.5 Hydraulic System

The two transmission mounted hydraulic pumps act as the primary hydraulic systems and power the flight control systems. The hydraulic pumps mounted on the auxiliary propulsion engines power the flight control surfaces on the wings and tail, auxiliary propulsion propeller pitch control actuators, and provide power to the utility system. If both transmission mounted hydraulic pumps fail the auxiliary propulsion hydraulic pumps can power the flight controls in a degraded (less responsive) mode. Two separate

yet functionally redundant logic control systems provide the cross-over and shut-off requirements.

11.2.6 Fuel System

The bottom of each sponson fuel tank is ballistically tolerant to a 23mm HE round and is self-sealing. Each of the large tanks include integrated baffles to disperse hydraulic ram. The suction type fuel pumps mounted on each engine deliver fuel through tear and cut resistant fuel lines. All fuel lines that run through the cargo compartment are self-sealing. This reduces fuel system leakage in the cargo area in event of a rupture. The fuel system is cross-feed capable.

11.2.7 Structure

The bottom of the fuselage is reinforced with several KEVLAR plates to protect critical components and structural members. Traditional semi-monocoque construction is used to distribute flight and cargo loads and a wing box is used to attach the wing to the fuselage. High strength composites make up the majority of the fuselage and empennage structure. Skin doublers are used in especially critical load convergent zones and high shear areas. Fairings and non-load bearing areas are constructed using KEVLAR impregnated composites tolerant to 12.7mm round fragments.

12. COST ANALYSIS

Programmatic difficulties and political pressures have placed a new emphasis on research, engineering, and development cost. The focus of this section is to provide a preliminary estimate of the *Condor's* cost. It is expected that the *Condor* will utilize existing technology wherever possible. Research and Development cost are not included in the scope of this estimation and no production trade-off analysis was attempted for this aircraft design. The *Condor* will use commercial off-the-shelf (COTS) components extensively in the avionics and flight control subsystems.

Undoubtedly, a corporate team will have to be formed to effectively and efficiently development and manufacture the *Condor*. This industry partnership would allow the cost and risk to be carried by several members, rather than just one. Each member would be challenged to minimize cost and to keep the cycle time short, thereby keeping the *Condor* affordable, both in design and production.

12.1 COST ESTIMATION METHOD

The cost estimation method used by the *Condor* design team is based on total recurring manufacturing cost per pound by major subsystem category. Cost figures were derived from past design reports, most notably the June 1993 *Arapaho* and June 1995 *Hakowi* design reports. This method is based on total recurring manufacturing cost per pound by major design subsystem. A composite factor was applied to the cost per pound figures if a subsystem contained a significant portion (>10%) of composite materials. The manufacturing recurring cost includes:

finished material plus material handling overhead and floor shrinkage; direct fabrication, assembly, and test cost plus overhead; quality assurance plus overhead.

Final recurring production cost estimates required an additional 40% for general and administrative (G&A) cost, cost-of-money (COM), and profit. An additional 35% was added to the total for inflation since cost data was based on 1992 dollars. This method resulted in an initial recurring manufacturing cost of **$126,385,113.25** per aircraft; a detailed breakdown is shown in Table 12.1.1, Cost Estimation Breakdown.

Table 12.1.1: Cost Estimation Method

	Recurring Manufacturing Cost - $/lb	Group weight - lbs	Composite Factor - 1.5 x cost/lb	Cost
Rotor	$1,400.00	10156.9	C	$21,329,497.96
Tail rotor	$1,400.00	1835.2	C	$3,853,971.77
Airframe (includes fuselage, tail boom, and empennage)	$760.00	15185.8	C	$17,311,862.10
Alighting gear	$220.00	2264.6		$498,208.25
Nacelle	$760.00	4861.3	C	$5,541,858.09
Propulsion w/APU (hp)	$300.00	27800.0	per hp	$8,340,000.00
Drive System (with transmission)	$325.00	11408.6		$3,707,787.64
Flight Controls	$220.00	232.0		$51,045.46
Instruments	$220.00	1714.5		$377,194.65
Hydraulic	$1,400.00	306.4		$428,930.60
Electrical	$270.00	722.7		$195,119.86
Avionics	$4,300.00	400.0		$1,720,000.00
Furnishing and equipment	$300.00	5368.2		$1,610,466.41
Door Mechanism	$450.00	1000.0		$450,000.00
Air Cond & anti ice	$1,400.00	938.4		$1,313,730.64
Manufacturing variation	$300.00	469.2		$140,756.85
			SUB-TOTAL	**$66,870,430.29**
			G & A, COM, PROFIT 40%	**$26,748,172.12**

INFLATION 35%	**$32,766,510.84**
TOTAL	**$126,385,113.25**

12.2 PRODUCTION COST FOR 100 UNITS

Total acquisition assumes an average production rate of 10 aircraft per year, a production run of 10 years, a cost improvement curve of 85%, and a recurring production cost of $126,385,113.25. The production cost is comprised by the cost of 33 aircraft costing $126,385,113.25, 34 aircraft costing $107,427,000 (.85), and 33 aircraft $90,997,300 (.72). Total production cost is $10,826,149,000. Table 12.2.1 summarizes unit and total cost.

Table 12.2.1: Production Cost

Production Size	Cost Improvement Rate	Price
33	1	$4,170,708,737.41
34	0.85	$3,652,529,773.06
33	0.72	$3,002,910,290.93
	TOTAL	$10,826,148,801.41

12.3 DIRECT OPERATING COST (DOC) ESTIMATE

A DOC analysis was not completed for the *Condor*.

LIST OF REFERENCES

[1] Prouty, Raymond, ***Helicopter Performance, Stability, and Control***, Krieger Publishing Company, 1995.

[2] Helicopter Design Team June 1993, ***Design of Arapaho, AHX***, Design Report, Naval Postgraduate School, Monterey, California, June 1993.

[3] Helicopter Design Team June 1995, ***Design of Hakowi,*** Design Report, Naval Postgraduate School, Monterey, California, June 1995.

[4] Helicopter Design Team June 1998, ***Design of Lakota,*** Design Report, Naval Postgraduate School, Monterey, California, June 1998.

[5] Dr. Jan Roskam, ***Airplane Design, "Part II: Preliminary Configuration Design and Integration of the Propulsion System"***, DARcorporation, 1997.

[6] Ira H. Abbott and Albert E. Von Doenhoff, ***Theory of Wing Sections***, Dover Publications Inc., 1959.

[7] Michael C.Y. Niu, ***Composite Airframe Structures***, Conmilt Press Ltd, Hong Kong, 1992.

[8] G.I. Zagainov and G.E. Lozino-Lozinski, ***Composite Materials in Aerospace Design***, Chapman & Hall, UK, 1996.

APPENDIX A WEIGHT ESTIMATE EQUATIONS

Main rotor blades

$$W_{b_M} = 0.026 b^{.66} c R^{1.3} (\Omega R)^{.67}$$

Main rotor hub and hinge

$$W_{h_M} = 0.0037 b^{.28} R^{1.3} (\Omega R)^{.43} \left(.67 W_{b_M} + \frac{gJ}{R^2}\right)^{.55}$$

Stabilizer (horizontal)

$$W_H = .72 A_H^{1.2} \text{A.R.}_H^{.32}$$

Fin (Vertical stabilizer)

$$W_V = 1.05 A_V^{.94} \text{A.R.}_V^{.53} (\text{no. of tail rotor gearboxes})^{.71}$$

Tail rotor

$$W_T = 1.4 R_T^{.090} \left(\frac{\text{Transmission h.p. rating}}{\Omega_M}\right)^{.90}$$

Body (fuselage)

$$W_F = 6.9 \left(\frac{\text{G.W.}}{1{,}000}\right)^{.49} L_F^{.61} (S\text{wet}_F)^{.25}$$

Landing gear

$$W_{\text{L.G.}} = 40 \left(\frac{\text{G.W.}}{1{,}000}\right)^{.67} (\text{No. of wheel legs})^{.54}$$

(add 10% for retraction)

Nacelles

$$W_N = 0.041 (\text{Total dry engine wt})^{1.1} (\text{No. of engines})^{.24} + 0.33\ (S\text{wet}_N)^{1.5}$$

Engine installation

$$W_{\text{eng}} = (\text{Installed wt. per eng.})(\text{No. of eng.})$$

Propulsion subsystems

$$W_{P.SS} = 2(W_{\text{eng}})^{.59} (\text{No. of eng.})^{.20}$$

Fuel system

$$W_{\text{F.S.}} = .43 (\text{cap. in gal.})^{.77} (\text{No. of tanks})^{.59}$$

Drive system

$$W_{\text{D.S.}} = 13.6 (\text{Transmission h.p. rating})^{.82} \left(\frac{\text{rpm}_{\text{eng}}}{1{,}000}\right)^{.057} \times \left[\left(\frac{\text{Tail rotor h.p. rating}}{\text{Transmission h.p. rating}}\right)\left(\frac{\Omega_M}{\Omega_T}\right)\right]^{.068} \frac{(\text{No. of gearboxes})^{.066}}{\Omega_M^{.64}}$$

Cockpit controls

$$W_{\text{C.C.}} = 11.5 \left(\frac{\text{G.W.}}{1{,}000}\right)^{.40}$$

(Triple if no boost is used)

Systems controls (boosted)

$$W_{\text{S.C.}} = 36 b_M c_M^{2.2} \left(\frac{\Omega R_M}{1000}\right)^{3.2}$$

Auxiliary power plant

$$W_{\text{A.P.P.}} = 150$$

(1980 state-of-the-art)

Instruments

$$W_T = 3.5 \left(\frac{\text{G.W.}}{1{,}000}\right)^{1.5}$$

Hydraulics

$$W_{\text{hyd.}} = 37 b_M^{.63} c^{1.5} \left(\frac{\Omega R_M}{1{,}000}\right)^{2.1}$$

Electrical

$$W_{\text{EL.}} = \frac{9.6 (\text{Transmission h.p. rating})^{.65}}{\left(\frac{\text{G.W.}}{1{,}000}\right)^{.40}} - W_{\text{hyd}}$$

Avionics

$$W_{\text{av.}} = \begin{cases} 50 \text{ (low)} \\ 150 \text{ (avg)} \\ 400 \text{ (high)} \end{cases}$$

Furnishings and equipment

$$W_{\text{FE}} = \begin{cases} 6 \left(\frac{\text{G.W.}}{1{,}000}\right)^{1.3} \text{ (low)} \\ 13 \left(\frac{\text{G.W.}}{1{,}000}\right)^{1.3} \text{ (avg)} \\ 23 \left(\frac{\text{G.W.}}{1{,}000}\right)^{1.3} \text{ (high)} \end{cases}$$

Air cond. & anti-ice

$$W_{\text{AC\&AI}} = 8 \left(\frac{\text{G.W.}}{1{,}000}\right)$$

Manufacturing variation

$$W_{\text{M.V.}} = 4 \left(\frac{\text{G.W.}}{1{,}000}\right)$$

Figure 2.1.1: Top view of *Condor*

Figure 2.1.2: Front view of *Condor*

Figure 2.1.3: Side view of *Condor*